SLAC – PUB – 3538
December 1984
T/E

Systematics of πN Scattering in Chiral Soliton Models

MICHAEL P. MATTIS AND MICHAEL E. PESKIN*

Stanford Linear Accelerator Center

Stanford University, Stanford, California, 94305

ABSTRACT

We study the spin and isospin structure of pion-nucleon scattering amplitudes in the class of models, including the Skyrme model, in which the nucleon arises as a soliton built of pion fields. We derive general linear relations among partial-wave amplitudes for the processes $\pi N \to \pi N$ and $\pi N \to \pi \Delta$ and show that these relations are in reasonably good agreement with experiment.

Submitted to *Physical Review D*

* Work supported by the Department of Energy, contract DE – AC03 – 76SF00515.

1. Introduction

It is now over a decade since 't Hooft first proposed that we might learn much about the strong interactions by studying a world in which the underlying gauge group is $SU(N)$ with N very large. This world is populated with an infinity of meson states in each J^{PC} channel; these mesons are stable and noninteracting in the $N \to \infty$ limit, with decay widths and 2-body scattering amplitudes which vanish as N^{-1} and N^{-2}, respectively. When N is large but finite, meson interactions are governed by the exchange, not of quarks and gluons, but of single mesons and glueballs, so that meson processes can be described by the tree-level diagrams of an "effective Lagrangian" of the sort that was extensively studied in the 1960's[1] . For the special case of the pseudoscalar mesons, chiral symmetry constrains the form of this Lagrangian to:

$$\mathcal{L} = \frac{f_\pi^2}{16} \mathrm{Tr}\,(\partial_\mu U \partial^\mu U^\dagger) + \cdots, \tag{1.1}$$

where U takes values on the group $SU(n_f)$ with n_f the number of light flavors. In this paper we shall specialize to the case $n_f = 2$. The parameter N enters in (1.1) through the pion decay constant f_π, which is proportional to $N^{\frac{1}{2}}$ in the large-N limit.

Recent years have seen mounting evidence that the baryons of the large-N world may be thought of as solitons of some effective meson Lagrangian[2,3] . At a first level, solitons typically have masses that diverge like the inverse of the coupling constant; likewise baryons, which are composed of N quarks, have $m \sim N = 1/N^{-1}$. In contrast, the size and shape of a soliton have smooth, nontrivial limits for vanishing coupling constant; this is the case for baryons as

well when $N \to \infty$. Most strikingly, as first noticed by Skyrme[4] , systems such as (1.1) based on a dynamical variable $U(x) \in SU(n_f)$ do indeed possess topologically stable solitons whose additive topological charge may be identified with baryon number (analogous statements hold for the effective meson theories which follow from other underlying gauge groups). It was shown long ago that these solitons can be quantized as fermions[5] . In fact, when $n_f \geq 3$ and the effect of QCD anomalies is properly taken into account in (1.1), one can prove a stronger statement: The soliton *must* be treated as a fermion when N is odd and as a boson when N is even, just as one would expect from the quark model. These points and others are discussed in detail in Refs. 2 and 3.

In this paper we shall examine some implications of this "chiral soliton" ansatz for the real world. At leading order in $1/N$, this ansatz implies a set of energy-independent linear relations between pion-nucleon scattering amplitudes in various channels of isospin and angular momentum, as recently noted by Hayashi *et al.*[6] in their analysis of πN scattering in the Skyrme model. These relations can be used, for example, to express the isospin-$\frac{3}{2}$ πN elastic scattering amplitudes as linear combinations of the isospin-$\frac{1}{2}$ amplitudes in the same partial wave; this comparison as applied to the experimental scattering data is depicted in the graphs of Fig. 2. Similar relations will be shown to hold for the process $\pi N \to \pi\Delta$. We shall find that in Nature these relations seem to be satisfied fairly well for most partial waves. Furthermore we shall argue that the handful of channels for which the relations are grossly disobeyed are precisely the ones most sensitive to higher-order corrections, which we have not attempted to calculate.

In addition, we shall find that the soliton interpretation of baryons provides a coherent framework for understanding some general features of the $\pi N \to \pi N$ partial wave amplitudes. In particular it offers a simple explanation for a surprisingly consistent pattern that emerges for when the four independent amplitudes in a given partial wave L are compared: namely, the amplitudes corresponding to $(I,J) = (\frac{1}{2}, L-\frac{1}{2})$ or $(\frac{3}{2}, L+\frac{1}{2})$ are characterized by much bigger excursions through the unitarity circle than those with $(I,J) = (\frac{1}{2}, L+\frac{1}{2})$ or $(\frac{3}{2}, L-\frac{1}{2})$. (Here I and J denote the total isospin and angular momentum of the pion-nucleon system.) Furthermore, the chiral soliton picture gives an intuitive understanding for why the S-, P- and D-waves are characterized both by enormous, low-lying resonances in some channels and marked repulsive behavior near threshold in others.

We begin our exposition in Section 2 with a general discussion of πN scattering in the large-N limit. Here we set out our approximations and justify them as appropriate to a systematic analysis to leading order in $1/N$. In Section 3, we employ these approximations to derive the general structure of the spin- and isospin-dependence of πN amplitudes implied by the $1/N$ expansion. Our results agree with those obtained in Ref. 6 by somewhat different means; the lengthier derivation given here has the advantage of highlighting the various points at which we invoke the large-N approximation, which we hope will help pave the way for a higher-order calculation. We recover the linear relations of Ref. 6 for elastic scattering and present new relations among partial wave amplitudes for the process $\pi N \to \pi\Delta$. We then apply these relations to the experimentally determined partial wave amplitudes, considering $\pi N \to \pi N$ and $\pi N \to \pi\Delta$ in Sections 4 and 5, respectively. The casual reader is encouraged to skip directly

to the linear relations (Eqs. (3.22)-(3.25)) and their discussion, and to peruse the justaposed graphs of Fig. 2.

The group-theoretic results of Section III are put to different use in Ref. 7 to obtain the elastic πN partial-wave amplitudes and, correspondingly, the full spectrum of nucleon and delta resonances in the specific context of the Skyrme model[4] . The results of that paper are on the whole in surprisingly good agreement with experiment for total energies up to 3 GeV. For the case of the F-waves, this agreement was already noted in Ref. 6.

2. Assumptions, Approximations, and Apologies

Most of the approximations we will make relate in one way or another to the large-N expansion. Our major approximation will be that of deriving the $\pi N \to \pi N$ and $\pi N \to \pi \Delta$ amplitudes from the lowest-order pion propagator in the (appropriately rotated) soliton background, ignoring all loop contributions to the two-point function. Loop diagrams necessarily contain 3-meson, 4-meson or higher-order vertices which are damped by increasingly higher powers of $f_\pi^{-1} \sim N^{-\frac{1}{2}}$. Consequently, all loop contributions to the propagator are suppressed by at least one power of N and can therefore be disregarded in our lowest-order treatment.

The fact that the bare pion propagator has enough structure to lead to non-trivial scattering is noteworthy and deserves some comment. On the one hand, this should be expected from the soliton picture, since meson-soliton scattering normally appears at zeroth order in a weak-coupling expansion. On the other hand, this fact implies that, in large-N, baryon resonances are not at all the

counterparts of excited mesons. As we have already noted, the widths of all excited mesons vanish like N^{-1} as $N \to \infty$. Among the baryons found in Nature, however, only the nucleon and delta (and perhaps a handful of others: see Section 4) appear as sharply defined states in this limit. Higher-mass baryons cannot be identified with narrow states; they appear only as resonances above threshold in the various channels of pion-nucleon scattering. The widths of these baryons are determined by the motion of the πN phase shifts in the relevant partial waves; since the equations for πN scattering have a definite, finite large-N limit, both the widths and the excitation energies of these resonances will be of order N^0. This picture contrasts sharply with the quark model description of baryon resonances. One may think of the quark model as representing the leading term in a nonrelativistic approximation to the baryon and meson states. In this limit, unlike that of large N, the baryon resonances appear as eigenstates of a Hamiltonian and hence are *stable* to lowest order. The first nonzero contribution to their widths arises from the corrections to this approximation involving the creation of extra quark-antiquark pairs.

The major limitation of our lowest-order large-N analysis is that it is appropriate only to elastic or quasielastic πN scattering. Multiple production of pions is formally suppressed by powers of $1/N$; nevertheless, in Nature it becomes the dominant feature of πN scattering at high energies. Our analysis, on the other hand, allows a pion to scatter inelastically from a nucleon only by producing a rotationally excited state of the soliton. This may be a delta, with $I = J = \frac{3}{2}$, or a specific higher excitation, peculiar to chiral soliton models, with $I = J = \frac{5}{2}$, as discussed further in Section 3.

Our second approximation will consist of ignoring the rotation of the soliton

during the scattering process. As we shall review below, nucleons and deltas correspond in the chiral soliton models to *rotating* solitons[8] of angular momentum $\mathbf{J}^2 = i(i+1)$, with $i = \frac{1}{2}$ and $i = \frac{3}{2}$, respectively. The nucleon-delta mass-difference is then simply due to to the rotational kinetic energy term $\mathbf{J}^2/2I$, where I denotes the moment of inertia of the soliton. Since $I \sim N$ this mass splitting is a $1/N$ effect. The rotational frequency of the soliton is then given by $\omega = J/I$, which likewise vanishes like $1/N$ for large N, thereby justifying our approximation in this limit.

This argument might not appear particularly compelling when applied to the real world, where $N = 3$. However one can reverse the above relations and solve for ω in terms of m_N and m_Δ; the result is $\omega = \frac{2}{3}J(m_\Delta - m_N)$. The ratio of the time it takes a pion of velocity v to cross the charge radius R of a nucleon to the period of rotation of the nucleon viewed as a soliton is then $(v/c)^{-1}(\omega R/2\pi)$ $\approx \frac{1}{16}(v/c)^{-1}$, while the corresponding ratio in the case of the delta is roughly $\frac{1}{5}(v/c)^{-1}$. Thus our approximation appears to be a reasonable one for $\pi N \to \pi N$ except near threshold, whereas for $\pi N \to \pi\Delta$ it is somewhat more severe.

Finally, we will ignore both the deformation and the recoil of the soliton. This, too, is formally justified for large N, since in this limit the baryon is much more massive than the pion. But in Nature this would seem to be a drastic assumption if one wants to go up to typical resonance energies, say 1700 MeV. Curiously, the linear relations among $\pi N \to \pi N$ scattering amplitudes work better and better for higher energies for a reason that has nothing to do with the validity of the large N limit; we will discuss this point in Section 4. But it is remarkable that in the Skyrme-model calculation of Ref. 7, in which the same approximations are invoked, locations of resonances of very high mass (up to 3

GeV) are, if anything, obtained more accurately than for the lighter ones.

For $\pi N \to \pi\Delta$ this last approximation is even harder to justify. In that case, the linear relations derived in Section 3 are only valid on an unphysical line in momentum space for which, not only are the initial and final baryons both at rest, but in addition the momenta of the incoming and outgoing pions are equal. When the final baryon is a nucleon we can get arbitrarily close to this line by considering pions sufficiently near threshold, but this is obviously not the case when the final baryon is a delta.

3. Derivation of Linear Relations

We begin our analysis of pion-nucleon scattering from the assumption that the solitons associated with the Lagrangian (1.1) have the "hedgehog" form[4,3] :

$$U_\circ(\vec{x}) = e^{iF(r)\hat{\mathbf{r}}\cdot\vec{\sigma}} \tag{3.1}$$

If $F(r)$ tends to 0 as $r \to \infty$ and to π as $r \to 0$, this defines a configuration with topological charge (which we identify with baryon number) equal to unity. This configuration is maximally symmetric in the sense that, although it is not invariant with respect to isospin or spatial rotations separately, it is invariant under a combination of space and isospace rotations.

We shall use the symbols $\vec{i}$ and $\vec{s}$ to denote the isospin and angular momentum of the baryon alone, and reserve $\vec{I}$ and $\vec{J}$ for the pion-baryon system, *i.e.*, $\vec{I} = \vec{i} + \vec{I}(pion)$ and $\vec{J} = \vec{s} + \vec{L}(pion)$. In this notation, the soliton is transformed both by $\vec{i}$ and by $\vec{s}$, but is preserved by $\vec{i} + \vec{s}$. We shall see the significance of this peculiar symmetry in a little while, when we consider the expansion of

$\mathcal{L}$ about the chiral soliton and identify the fluctuations with pions; the result is that the pion wavefunctions decompose into eigenstates of the operator $\vec{K} \equiv \vec{I}(pion) + \vec{L}(pion)$. For the moment, however, let us return to the question of identifying the soliton with a physical baryon.

As it stands, $U_\circ$ is not a suitable candidate for a nucleon or delta; this is because physical baryons are characterized by definite values of $\vec{i}$ and $\vec{s}$ *individually.* In order to establish our notation we shall take this opportunity to review, in first-quantized language, the construction of nucleons and deltas that was presented in second-quantized form in Ref. 8. This construction begins with the realization that (3.1) picks out only one of an infinite class of possible orientations between spin and isospin axes; equally acceptable soliton solutions of (1.1) are furnished by

$$U_A \equiv A_{(\frac{1}{2})} U_\circ A^{-1}_{(\frac{1}{2})} \equiv e^{iF(r)(A_{(1)}\hat{r})\cdot\vec{\sigma}} \tag{3.2}$$

where A is any (constant) $SU(2)$ group element with spin-$\frac{1}{2}$ and spin-1 representations $A_{(\frac{1}{2})}$ and $A_{(1)}$. The natural action of isospin and angular momentum on this rotated soliton is given by:

$$\begin{aligned} \text{Isospin}: \quad & U_A \to U_I A_{(\frac{1}{2})} U_\circ A^{-1}_{(\frac{1}{2})} U_I^{-1} \\ \text{Angular Momentum}: \quad & U_A \to A_{(\frac{1}{2})} U_J^{-1} U_\circ U_J A^{-1}_{(\frac{1}{2})} \end{aligned} \tag{3.3}$$

It is fruitful at this point to think of A as a quantum-mechanical variable that takes values on the group manifold $SU(2)$. A suitable candidate for a physical baryon is then a coherent superposition

$$\int dA\, \chi(A)\, |A\rangle\,. \tag{3.4}$$

Here dA represents the group-invariant measure, normalized so that $\int dA = 2\pi^2$;

$|A\rangle$ is the state containing a soliton in the orientation U_A; and the wavefunction $\chi(A)$ is chosen appropriately to make this expression an eigenstate of both $\vec{i}$ and $\vec{s}$. Because U_0 is invariant under $\vec{i}+\vec{s}$, (3.4) will always have $i = s$. One may think of this expression as describing a *rotating* soliton.

The construction of the wavefunctions $\chi(A)$ corresponding to definite states of (i, i_z) and (s, s_z) is a straightforward exercise[8] . For nucleons (with $i = s = \frac{1}{2}$) one finds

$$\chi^{(\frac{1}{2})}_{i_z s_z}(A) = \frac{i}{\pi}\left(\epsilon_{(\frac{1}{2})} A^{-1}_{(\frac{1}{2})}\right)_{s_z i_z} \quad ; \quad \epsilon_{(\frac{1}{2})} = \begin{pmatrix} 0 & 1 \\ -1 & 0 \end{pmatrix}, \tag{3.5}$$

while a general rotational eigenstate, with $i = s = R$, has as its properly normalized wavefunction[♯1] :

$$\chi^{R}_{i_z s_z}(A) = \frac{i}{\pi}\sqrt{\frac{1}{2}(2R+1)}\left(\epsilon_{(R)} A^{-1}_{(R)}\right)_{s_z i_z} . \tag{3.6}$$

Note that these wavefunctions are really only appropriate for baryons at rest; however, as we have discussed in Section 2, we will in any event neglect the baryon's recoil in the scattering process.

Let us turn next to the question of how to represent pion field fluctuations about the classical soliton. It is easiest to begin by considering the soliton in its canonical orientation (3.1). One can then allow pion fluctuations about the soliton by letting $F(r)\hat{\mathbf{r}} \to F(r)\hat{\mathbf{r}} + \frac{2}{f_\pi}\vec{\pi}(\vec{x}, t)$ in the exponent. Expanding (1.1) in

♯1 Of course, for each R, we have the freedom to redefine the wavefunctions $\chi^R_{i_z s_z}$ by a common phase; our choice agrees with Ref. 8 for the nucleons but differs by a sign for the deltas, in order to conform in this case to Ref. 9. A different phase convention modifies the linear relation (3.25) below.

powers of the pion field yields an action

$$S = -m_\circ + \int d^4x\, \pi^{i*}(x)\widehat{\mathbf{L}}_{ij}\pi^j(x) + O(\pi^3/f_\pi), \tag{3.7}$$

where $m_\circ$ is the mass of the soliton and i and j are isospin indices that we shall think of as running over $(1,2,3)$ or $(+,0,-)$ as convenient (the latter basis requiring complex conjugation in (3.7), as well as in the associated Green's function (3.10) below). $\widehat{\mathbf{L}}$ is accordingly a 3×3 matrix of differential operators formed from various products of $\partial_i, \partial_t^2, \hat{\mathbf{r}}_i$ and δ_{ij}. That is,

$$\widehat{\mathbf{L}}_{ij} = G_1(r)\delta_{ij} + G_2(r)\delta_{ij}\partial_t^2 + G_3(r)\hat{r}_i\hat{r}_j\partial_t^2 + G_4(r)\,\hat{r}_j\partial_i + G_5(r)\hat{r}_i\partial_j + \cdots \tag{3.8}$$

with the $G_k(r)$ being, in general, horrible, model-dependent functions of the soliton profile $F(r)$ and its derivatives[#2] . We note that, with no loss of generality, $\widehat{\mathbf{L}}$ can be chosen uniquely to be self-adjoint. As discussed in Section 2, we shall henceforth neglect all $O(\pi^3/f_\pi)$ terms in keeping with our lowest-order approach.

We can now imagine constructing the pion propagator $\langle \pi^i(\vec{x}',t')\pi^j(\vec{x},t)\rangle_\circ$ in the soliton background by the following procedure: The pion field is expanded in terms of a complete set of appropriately normalized eigenfunctions $\psi^j_\lambda(\vec{x},t)$ satisfying

$$\widehat{\mathbf{L}}_{ij}\psi^j_\lambda = a(\lambda)\,\psi^i_\lambda \tag{3.9}$$

The propagator is then given, somewhat schematically, by

$$\left\langle \pi^i(x')\pi^j(x)\right\rangle_\circ = \sum_\lambda \frac{\psi^i_\lambda(x')\psi^j_\lambda(x)}{a(\lambda)}\ . \tag{3.10}$$

Note that by time-reversal invariance $\widehat{\mathbf{L}}$, hence also ψ_λ, is purely real when con-

[#2] The symbol ϵ_{ijk} is forbidden by parity; likewise derivatives of odd order in time are disallowed by time-reversal invariance.

sidered in the (1,2,3) basis. The 'nought' on the propagator will serve to remind us that (3.10) represents pion-scattering from a fixed soliton in its standard orientation (3.1).

It is obvious how to generalize this formula to the case of a rotated soliton U_A as defined in (3.2). Pion fluctuations are naturally incorporated by letting $F(r)A_{(1)}\hat{\mathbf{r}} \to F(r)A_{(1)}\hat{\mathbf{r}} + \frac{2}{f_\pi}\vec{\pi}(\vec{x},t)$ as before. This results in $\widehat{\mathbf{L}} \to A_{(1)}\widehat{\mathbf{L}}{A_{(1)}}^{-1}$, $\psi^j_\lambda \to A_{(1)jk}\psi^k_\lambda$, and thus

$$\left\langle \pi^i\pi^j \right\rangle_\circ \to \left\langle \pi^i\pi^j \right\rangle_A = A_{(1)im}\left\langle \pi^m\pi^n \right\rangle_\circ A^{-1}_{(1)nj}. \tag{3.11}$$

We should point out that this step assumes the rotation A to be time-independent; thus, it is valid only in the limit in which the soliton does not rotate significantly during the scattering process. This approximation was justified in Section 2 as arising from the $1/N$ expansion.

It is now a simple matter to express in this framework the Green's functions for the "real-world" processes $\pi N \to \pi N$ and $\pi N \to \pi\Delta$. If we represent the initial and final baryons by the wavefunctions $\chi^R_{i_z s_z}(A)$ and $\chi^{R'}_{i'_z s'_z}(A)$, respectively, then the Green's functions are given by

$$\left\langle \pi^i\pi^j \right\rangle = \int dA\, \chi^{R's}_{i'_z s'_z}(A)A_{(1)im}\left\langle \pi^m\pi^n \right\rangle_\circ A^{-1}_{(1)nj}\chi^R_{i_z s_z}(A) \tag{3.12}$$

$$= \frac{1}{2\pi^2}\sqrt{(2R+1)(2R'+1)}\sum_{mn}\left\langle \pi^m\pi^n \right\rangle_\circ$$

$$\times \int dA\big(A_{(R')}\epsilon^{-1}_{(R')}\big)_{i'_z s'_z}A_{(1)im}{A_{(1)}}^{-1}_{nj}\big(\epsilon_{(R)}A^{-1}_{(R)}\big)_{s_z i_z}$$

where we have substituted the explicit expressions for the baryon wavefunctions given in (3.6).

It turns out that the A-integration in Eq. (3.12) can be carried out explicitly. The most compact expression for the Green's function is then obtained by projecting the initial and final pion-baryon states onto states of definite total isospin and angular momentum $|II_zJJ_z\rangle$. ($\vec{I}$ and $\vec{J}$ are of course conserved in the scattering process.) Furthermore we restrict the incoming and outgoing pions to partial waves L and L', respectively, while the initial and final baryons are characterized by spin (and isospin) R and R' as before. These steps are carried out in detail in Appendix A. The appropriately projected pion Green's functions, which we label $\mathbf{G}_{LL'RR'\vec{I}\vec{J}}(rt;r't')$, are then given by an expression of the form:

$$\mathbf{G}_{LL'RR'\vec{I}\vec{J}} = \sum_K P_{LL'RR'IJK} \cdot \mathbf{g}_{KL'L}(rt;r't') \tag{3.13}$$

The meanings of the terms on the right-hand side of this expression are as follows: $\mathbf{g}_{KL'L}(rt;r't')$ is the "reduced" radial Green's function describing elastic pion-scattering from the "elementary" soliton (3.1), where the incoming and outgoing pions are restricted to partial waves L and L', respectively; this restriction leaves a purely radial scattering problem. The index K denotes the conserved quantum number of this "elementary" process, which is the vectorial sum $\vec{K} = \vec{I}(pion) + \vec{L}(pion)$. Note that, by the triangle inequality, K is restricted to the values $\max(|L-1|,|L'-1|) \leq K \leq \min(L+1, L'+1)$. Finally, the P-symbols are group-theoretic coefficients calculated in Appendix A:

$$P_{LL'RR'IJK} = (-1)^{R'-R}\sqrt{(2R+1)(2R'+1)}(2K+1)\begin{Bmatrix} KIJ \\ R'L'1 \end{Bmatrix}\begin{Bmatrix} KIJ \\ RL1 \end{Bmatrix}. \tag{3.14}$$

The appearance of $6j$-symbols in this expression is quite natural, since, as indicated in Fig. 1, the problem in both the entering and the exiting πN channels

is characterized by six intertwined angular momenta. Explicit formulas for the P-symbols relevant to $\pi N \to \pi N$ and $\pi N \to \pi \Delta$ are presented in Appendix B. Note that all the model dependence arising from the details of the Lagrangian (1.1) is subsumed in the quantities $g_{KL'L}$; the P-symbols, in contrast, depend only on the hedgehog nature of the chiral soliton.

Since $6j$-symbols embody various triangle inequalities, the same is true for the P-symbols. Specifically, the seven triads $(R1I)$, $(R'1I)$, (RLJ), $(R'L'J)$, $(L1K)$, $(L'1K)$ and (IJK) must each satisfy the triangle inequality in order for the P-symbol not to vanish (*cf.* Fig. 1). Of these triads, the first four merely express the obvious bounds on the total isospin and angular momentum formed from a baryon of spin and isospin R (or R') and a pion with orbital angular momentum L (or L').

As for $(L1K)$ and $(L'1K)$, these reflect the existence of the conserved vector $\vec{K}$ in processes in which a pion scatters off an elementary soliton. Indeed Eq. (3.13) can best be regarded as an expansion of the physical processes $\pi N \to \pi N$ or $\pi N \to \pi \Delta$ in terms of these elementary channels, each labeled by its own value of K. The emergence of this new quantum number as a quantity of physical import is of course peculiar to models that admit solitons of the form given in Eq. (3.1).

The final triad (IJK) is something of a surprise. (In fact it is the only one of the seven triangle inequalities not already manifest in the Clebsch-Gordon coefficients of Eq. (A.9), which is the penultimate formula in the derivation of (3.14).) In practice, it frequently serves to eliminate one of the (typically three) elementary channels associated with fixed K which would normally be expected to contribute to a given (I, J, L) channel of physical pion-baryon scattering.

Despite these restrictions it turns out that Eq. (3.14) does not prohibit any πN or $\pi\Delta$ processes otherwise allowed by parity, isospin, and angular momentum. For example, $(L1K)$ and $(L'1K)$ taken together forbid jumps in pion angular momentum greater than two; but $\Delta L \geq 3$ is in any event excluded by parity and/or angular momentum conservation. (Such would not be the case in a world where the color group were $SU(N)$ with $N > 3$. Suppose, for example, that N were seven. One would then expect to find well-defined baryons $B_{\frac{7}{2}}$ with $i = s = 7/2$; consequently jumps of four units of pion angular momentum in such processes as $\pi N \rightarrow \pi B_{\frac{7}{2}}$, although disallowed by (3.13), would nevertheless be consistent with angular momentum conservation.)

The relation (3.13) for Green's functions can be immediately converted to a relation for S-matrix elements by moving onto the pion mass-shell and extracting the pole term on each side of this equation. Modulo the extrapolation from an unphysical region in momentum-space as discussed in Sec. II, these manipulations do not change the form of the relation, and we have:

$$\mathbf{S}_{LL'RR'\vec{I}\vec{J}} \equiv^{+} \left\langle R'\vec{I}\vec{J}L'|R\vec{I}\vec{J}L\right\rangle^{-} = \sum_{K} P_{LL'RR'IJK} \cdot \mathbf{s}_{KL'L}. \tag{3.15}$$

We will refer to the $\mathbf{s}_{KL'L}$ as the *reduced* S-matrix. Notice that a resonance in some elementary channel (KLL') manifests itself in πN scattering as a family of resonances coupling to that value of K. It is thus appropriate in the chiral soliton picture to classify resonances according to K[10–13] . This scheme replaces the conventional $SU(6)$ classification of baryon resonances. We should recall, though, that these resonances should not be considered narrow, so that one may not ignore background contributions from other values of K coupling to the same physical partial wave amplitude.

As a check on (3.15) let us verify the unitarity condition

$$ {}^{+}\langle f|i\rangle^{-} = \sum_{\psi} {}^{+}\langle f|\psi\rangle^{\circ}\,{}^{\circ}\langle\psi|i\rangle^{-}, \tag{3.16} $$

where $|\psi\rangle^{\circ}$ runs over a complete set of states at an intermediate time. Accordingly we rewrite the reduced S-matrix as

$$ \mathbf{s}_{KL'L} \equiv \mathbf{s}^{+-}_{KL'L} \equiv {}^{+}\langle KL'|KL\rangle^{-} \tag{3.17} $$

and insert

$$ \sum_{R''L''} \left|R''\vec{I}\vec{J}L''\right\rangle^{\circ}\;{}^{\circ}\left\langle R''\vec{I}\vec{J}L''\right| \tag{3.18} $$

into (3.15). Taking advantage of the fact that

$$ \sum_{R''} P_{LL''RR''IJK'}P_{L''L'R''R'IJK} = \delta_{KK'}P_{LL'RR'IJK} \tag{3.19} $$

(which holds so long as the triad $(L''1K)$ satisfies the triangle inequality), we obtain the constraint

$$ \sum_{K} P_{LL'RR'IJK}\cdot(\mathbf{s}^{+-}_{KL'L} - \sum_{L''}\mathbf{s}^{+\circ}_{KL'L''}\mathbf{s}^{\circ-}_{KL''L}) = 0, \tag{3.20} $$

where we have set ${}^{+}\langle KL'|KL''\rangle^{\circ} = \mathbf{s}^{+\circ}_{KL'L''}$, etc. From this we can draw the reassuring conclusion that if the reduced S-matrix obeys (3.16) (as surely it must), then the physical amplitudes are guaranteed to do so as well.

Note, however, that it is generally necessary to include the "exotic" baryons with $R'' > 3/2$ called for by the model among the states of the complete set

(3.18). This should not be surprising; the chiral soliton model contains a state of spin and isospin $\frac{5}{2}$ as the second rotational excitation of the nucleon, and there is no selection rule forbidding the production of this baryon in isospin-$\frac{3}{2}$ πN scattering, via the process $\pi N \to \pi B_{\frac{5}{2}}$. By analogy with the rigid rotor, the mass of this baryon would satisfy $(m_{\frac{5}{2}} - m_N)/(m_\Delta - m_N) = \frac{8}{3}$, or $m_{\frac{5}{2}} \simeq 1720$ MeV. Of course, in Nature there is no such state narrow enough to be distinguished. It is nevertheless conceivable that a very broad $i = s = \frac{5}{2}$ resonance exists. Presumably it would decay mostly into $\Delta\pi$ and would therefore show up obliquely in Nature as an enhancement of the $\Delta\pi\pi$ (or $\Delta\rho$) final state in pion-nucleon scattering.

The obvious benefit of Eq. (3.15) is that it decomposes a large number of physical scattering amplitudes in terms of a substantially smaller set of reduced amplitudes. Consequently it is possible to eliminate the latter and be left with nontrivial energy-independent linear relations between physical amplitudes. Before doing so, however, we pause briefly to take note of two general constraints on the the reduced amplitude $s_{KL'L}$. First of all, parity conservation together with the triangle inequalities discussed above for $(L1K)$ and $(L'1K)$ imply that either $L = L'$ or $L = L' \pm 2$. Secondly, it follows from time-reversal invariance and unitarity that the S-matrix is symmetric[14] :

$$s_{KL'L} = s_{KLL'}. \tag{3.21}$$

Bearing these constraints in mind, we can now straightforwardly find linear combinations of the left-hand side of (3.15) so that the model-dependent right-hand side cancels out.

We focus first on the case $\pi N \to \pi N$; in our notation this implies $L = L'$ and $R = R' = \frac{1}{2}$. We choose to solve for the $I = \frac{3}{2}$ amplitudes in terms of those with $I = \frac{1}{2}$. From the explicit formulas for the P-symbols as given in Appendix B one obtains:

$$\mathbf{S}_{LL\frac{1}{2}\frac{1}{2}\frac{3}{2},L-\frac{1}{2}} = \frac{L-1}{4L+2} \cdot \mathbf{S}_{LL\frac{1}{2}\frac{1}{2}\frac{1}{2},L-\frac{1}{2}} \tag{3.22a}$$

$$+\frac{3L+3}{4L+2} \cdot \mathbf{S}_{LL\frac{1}{2}\frac{1}{2}\frac{1}{2},L+\frac{1}{2}}$$

and

$$\mathbf{S}_{LL\frac{1}{2}\frac{1}{2}\frac{3}{2},L+\frac{1}{2}} = \frac{3L}{4L+2} \cdot \mathbf{S}_{LL\frac{1}{2}\frac{1}{2}\frac{1}{2},L-\frac{1}{2}} \tag{3.22b}$$

$$+\frac{L+2}{4L+2} \cdot \mathbf{S}_{LL\frac{1}{2}\frac{1}{2}\frac{1}{2},L+\frac{1}{2}}$$

These relations were also derived in Ref. 6.

For $\pi N \to \pi \Delta$ we can have either $L = L'$ or $L = L' \pm 2$ consistent with angular momentum conservation. For $L = L'$ we find:

$$\mathbf{S}_{LL\frac{1}{2}\frac{3}{2}\frac{3}{2},L-\frac{1}{2}} = \frac{4(L-1)}{\sqrt{10}(2L+1)} \cdot \mathbf{S}_{LL\frac{1}{2}\frac{3}{2}\frac{1}{2},L-\frac{1}{2}} \tag{3.23a}$$

$$+\frac{3}{2L+1}\sqrt{\frac{(L+1)(2L+3)(2L-1)}{10L}} \cdot \mathbf{S}_{LL\frac{1}{2}\frac{3}{2}\frac{1}{2},L+\frac{1}{2}}$$

and likewise

$$\mathbf{S}_{LL\frac{1}{2}\frac{3}{2}\frac{3}{2},L+\frac{1}{2}} = \frac{3}{2L+1}\sqrt{\frac{L(2L+3)(2L-1)}{10(L+1)}} \cdot \mathbf{S}_{LL\frac{1}{2}\frac{3}{2}\frac{1}{2},L-\frac{1}{2}} \tag{3.23b}$$

$$+\frac{4(L+2)}{\sqrt{10}(2L+1)} \cdot \mathbf{S}_{LL\frac{1}{2}\frac{3}{2}\frac{1}{2},L+\frac{1}{2}},$$

while for $L = L' \pm 2$ we obtain the simple proportionality relations

$$\begin{aligned}\sqrt{L+1}\cdot \mathbf{S}_{L,L+2,\frac{1}{2}\frac{3}{2}\frac{1}{2},L+\frac{1}{2}} &= -\sqrt{10(L+1)}\cdot \mathbf{S}_{L,L+2,\frac{1}{2}\frac{3}{2}\frac{3}{2},L+\frac{1}{2}} \\ = -\sqrt{L+2}\cdot \mathbf{S}_{L+2,L\frac{1}{2}\frac{3}{2}\frac{1}{2},L+\frac{3}{2}} &= \sqrt{10(L+2)}\cdot \mathbf{S}_{L+2,L\frac{1}{2}\frac{3}{2}\frac{3}{2},L+\frac{3}{2}}.\end{aligned} \tag{3.24}$$

Finally, for each L there is one additional linear relation which serves to relate $\pi N \to \pi N$ to $\pi N \to \pi\Delta$:

$$\begin{aligned}&\mathbf{S}_{LL\frac{1}{2}\frac{1}{2}\frac{1}{2},L-\frac{1}{2}} - \mathbf{S}_{LL\frac{1}{2}\frac{1}{2}\frac{1}{2},L+\frac{1}{2}} \\ &\qquad = \sqrt{\frac{2L-1}{L+1}}\cdot \mathbf{S}_{LL\frac{1}{2}\frac{3}{2}\frac{1}{2},L-\frac{1}{2}} + \sqrt{\frac{2L+3}{L}}\cdot \mathbf{S}_{LL\frac{1}{2}\frac{3}{2}\frac{1}{2},L+\frac{1}{2}}\end{aligned} \tag{3.25}$$

(Note that this relation depends on the phase convention of the delta wavefunctions *vis-a-vis* the nucleons.)

We turn now to an examination of how well these relations are obeyed in Nature.

4. Comparison with Experiment: $\pi N \to \pi N$

We focus first on the process $\pi N \to \pi N$. Elastic πN scattering in the low-energy regime has been the subject of thorough experimental investigation. Our analysis in this section relies on the data compilation of Höhler, *et al.*,[15] in which a complete partial-wave analysis of elastic πN scattering is presented for center-of-mass energies W up to 4.5 GeV. For elastic scattering the relevant linear relations are given by Eq. (3.22), which expresses the isospin-$\frac{3}{2}$ amplitudes as linear combinations of the two isospin-$\frac{1}{2}$ amplitudes in the same partial wave. We now examine the experimental validity of these relations.

In Fig. 2, we display the experimental isospin-$\frac{3}{2}$ πN scattering amplitudes for $L \leq 7$ juxtaposed with those particular linear combinations of isospin-$\frac{1}{2}$ amplitudes to which they are predicted to correspond; these are indicated by solid and dashed lines, respectively. The closeness of these comparisons can be considered a model-independent test, not only of the chiral-soliton description of baryons, but also of the extent to which a lowest-order analysis in the $1/N$ expansion can be trusted to give a reasonable description of Nature. We should point out that, in keeping with tradition, our Argand plots depict the T-matrix; this is related to the S-matrix via $\mathbf{T} = \frac{1}{2i}(\mathbf{S} - \mathbf{1})$, with $\mathbf{1}$ denoting the identity operator on the Hilbert space (which vanishes for inelastic scattering).

The most striking feature of the graphs taken as a whole is the substantial qualitative agreement that one finds between theory and experiment, particularly for $L \geq 3$ (F-waves and higher). On a quantitative level, it turns out that, with few exceptions, the actual $I = \frac{3}{2}$ resonances are typically more massive by 150-300 MeV than predicted by the superposed $I = \frac{1}{2}$ amplitudes. This systematic splitting is presumably caused by the same rotational energy contribution that is responsible for the nucleon-delta mass difference; since this is a $1/N$ effect, it does not, indeed cannot, emerge in our lowest-order analysis. In contrast, it is apparent on the whole that the *shapes* of the resonances are correctly predicted by Eq. (3.22), and that the form of the backgrounds are reproduced quite satisfactorily. The correlation between the detailed structure of the F_{37} resonance and the corresponding linear combination $\frac{9}{14}F_{15} + \frac{5}{14}F_{17}$ is particularly remarkable. Note that the background contributions tend to be given correctly even in those low-L channels such as P_{33} for which the structure of the resonances is not reproduced well.

Having noted the generally high degree of agreement, it is of course important to confront the disappointing results in the S_{31}, P_{33} and D_{35} channels. It turns out that the poor agreement in these channels is not necessarily fatal to the chiral soliton ansatz. To see this, note that in each case the discrepancies are clearly the greatest near threshold. Now, it is a property of all chiral soliton models in which the soliton is of the 'hedgehog' form that the threshold behavior of the S-, P- and D-wave amplitudes (and *only* these amplitudes) is extremely sensitive to small perturbations. This point is argued at length in Ref. 7; we should briefly review that argument here.

The argument follows from the existence of rotational and translational zero-modes of the soliton which manifest themselves in lowest-order in $1/N$ as zero-excitation-energy boundstates in pion-nucleon scattering. Explicitly, these are given by

$$\mathbf{\Pi}_1^{1m}(\Omega)F(r) \tag{4.1a}$$

and

$$\mathbf{\Pi}_0^{1m}(\Omega)(F' + \frac{2F}{r}) + \mathbf{\Pi}_2^{1m}(\Omega)\sqrt{2}(\frac{F}{r} - F'), \tag{4.1b}$$

respectively, where $F(r)$ is the profile of the soliton (3.1), and $\mathbf{\Pi}_L^{KK_3}(\Omega)$ is the vector spherical harmonic defined in Appendix A. The subscripts denote the partial waves of πN scattering in which these boundstates appear; consequently the rotational zero-modes couple to the four P-wave channels, and the translational zero-modes to the six S- and D-waves.

When the pion mass is small, as it is in Nature, these degenerate boundstates lie only slightly below threshold. Now, this degeneracy is really only an artifact of

working to lowest order; in particular, the S-matrix poles corresponding to these zero-modes are inevitably perturbed away from their canonical location by terms which contribute in the next-leading order in the $1/N$ expansion. (The rotational energy responsible for the nucleon-delta mass-splitting is one such term.) Since on general grounds the behavior of the S-matrix in a given energy range is always strongly dependent on the precise position of nearby poles, we can conclude that the low-energy behavior of the S-, P- and D-wave πN amplitudes will be extremely sensitive to the details of the perturbations induced by these next-leading terms. For example, a small positive displacement of the pole into the fourth quadrant of the second sheet will result in the appearance of an enormous low-energy resonance, while, in sharp contrast, a small negative displacement of the pole, *i.e.* one which moves it away from the physical region, will produce only a (possibly repulsive) background contribution to the amplitude. (The reader is directed to Sec. III of Ref. 7 for further details.)

It is therefore completely unrealistic to expect a lowest-order calculation in $1/N$ such as ours to yield good agreement near threshold for the S-, P- and D-wave amplitudes. We find it encouraging that these are the only partial waves which are not in accord with Eq. (3.22) at low energies, and furthermore, that at higher energies (albeit still in the resonance region) the agreement markedly improves.

As evidence for this latter claim, consider Fig. 3, where we have plotted the speed of motion $|d\mathbf{T}/dW|$ of our prediction for the P_{33} partial wave amplitude as a function of the excitation energy ΔW; the maxima of the speed should give the positions of resonances. In Nature, this channel is characterized by three resonances, at 1232, 1522 and 1868 MeV. Our prediction likewise gives evidence

of three resonances, at 1360, 1780 and 2140 MeV; the shifts from Nature are of the order of $1/N$ corrections. The discrepancies at low energies evident in the juxtaposed graphs in this channel can be traced to the large difference in elasticity between the $\Delta(1232)$, in the true P_{33} channel, and the 'Roper resonance' $P_{11}(1410)$, which contributes to the comparison curve. Now, elasticity factors are measures of the phase-space of available decay modes; consequently, near thresholds they are extremely sensitive to small shifts in mass, and hence, to higher-order $1/N$ effects. We conclude that the agreement obtained in the P_{33} channel is as good as can reasonably be expected in a lowest-order treatment.

In fact, one might go so far as to assert, following Ref. 7, that the chiral soliton ansatz provides precisely the right framework for understanding why the S-, P- and D-wave amplitudes exhibit such a wide variety of behavior in the low-energy regime. Specifically, some channels are characterized by strong low-lying resonances (certainly the $P_{33}(1232)$, and arguably the $P_{11}(1410)$, $D_{13}(1519)$ and $S_{11}(1526)$ as well), while others, in complete contrast, are marked by repulsive behavior of the amplitudes near threshold (*cf.* the S_{31}, P_{31}, P_{13} and D_{35} channels). According to the scenario outlined above, the former would simply correspond to zero-mode poles which have been perturbed by higher-order effects into the fourth quadrant, while the latter would indicate that the poles had been pushed into the first or second quadrants. Note that, in this picture, the above-named resonances are considered to be heavier than the proton only by an amount of order $1/N$, whereas the usual resonances have excitation energies proportional to N^0. These resonances should also have parametrically small widths.

Before leaving the discussion of discrepancies in the low-lying partial waves, we should address the subject of the apparent violation of Weinberg's well-known

calculation[16] of the S-wave scattering-lengths[♯3] $a_{I=\frac{1}{2}}$ and $a_{I=\frac{3}{2}}$. The prediction is

$$a_{I=\frac{1}{2}} = -2a_{I=\frac{3}{2}} = \frac{g_V^2}{\pi f_\pi^2} \cdot \frac{m_\pi m_N}{m_\pi + m_N}, \tag{4.2}$$

which, in particular, correctly implies that the isospin-$\frac{1}{2}$ and isospin-$\frac{3}{2}$ S-wave amplitudes should exhibit attractive and repulsive behavior, respectively, near threshold. In contrast, the chiral-soliton prediction emerging from Eq. (3.22b) is that these amplitudes should be identically equal to one another! This is all the more disturbing in light of the result[17] that chiral soliton models must necessarily obey all soft-pion theorems, of which Weinberg's is a notable example.

Actually, there is no contradiction. To see this, recall that the equality of the amplitudes implied by (3.22b) is only valid to order N^0. To this order, as just discussed, the 'nearby' S-matrix poles in the two S-wave channels sit precisely on the real axis at the nucleon mass (where they have actually coalesced with zeroes of the S-matrix). Now, by elementary trigonometry, a phase-shift evaluated at a given value of energy is roughly proportional to the imaginary part of the nearby pole; this implies that, to lowest order, both $a_{I=\frac{1}{2}}$ and $a_{I=\frac{3}{2}}$ must vanish identically. And indeed, the right-hand side of Eq. (4.2) is manifestly of order $1/N$, with the result that Weinberg's prediction is trivially satisfied to order N^0. A nontrivial consistency check, then, must await a higher-order calculation.

We should comment further on the striking agreement apparent in all the channels depicted in Fig. 2 in the high-energy limit. Actually this agreement is something of an accident: in Nature, the four independent amplitudes in each

♯3 Recall that the S-wave T-matrix is related to the scattering length a near threshold via $\mathbf{T} = \frac{1}{2i}(\exp(2iak) - \mathbf{1})$, where k is the pion momentum.

partial wave become virtually degenerate at high energies (typically, $W \gtrsim 2800$ MeV), with the result that Eq. (3.22) is satisfied automatically. What we have, then, is in essence no more than a pleasing consistency check on our linear relations[♯4] .

In fact, one can argue that the $1/N$ expansion is no longer appropriate at high energies. In this regime, the πN total cross section is dominated by multiple production of pions. The elastic amplitude (which becomes characterized more and more by forward scattering) then arises as the shadow of this multiple production via the optical theorem. In the language of Regge theory, the elastic amplitude is dominated by Pomeron exchange. The couplings of the Pomeron are independent of spin and isospin orientation; this accounts for the degeneracy mentioned above. In any case, it is clear that these couplings, arising as they do from multiple pion production, depend simultaneously on many orders in $1/N$. Consequently, where the Pomeron dominates, a leading-order $1/N$ analysis is necessarily inadequate[♯5] .

We turn, finally, to what we consider the most compelling argument in favor of the chiral soliton ansatz that can be gleaned from an analysis of pion-nucleon scattering. We have just seen that, as the center-of-mass energy $W \to \infty$, the four independent amplitudes corresponding to each partial wave approach a common limit. However, for intermediate ranges of energy this is decidedly not the case. In fact, as pointed out in Ref. 7, when one restricts W to be ≤ 2.5 GeV the

---

♯4 It should be mentioned, however, that for the majority of channels the agreement in this region is closer by $30 - 50\%$ than what one would expect from comparing to a "random" (convex) linear combination.

♯5 It is therefore not surprising that explicit calculations of the partial-wave amplitudes in the specific case of the Skyrme model[6,7] grossly underestimate the inelasticity of πN scattering in all partial waves at high energy.

experimental Argand plots exhibit a strikingly consistent pattern: for each value of L, the excursion of the amplitude into the unitarity circle is nearly always much larger for the $(I,J) = (\frac{1}{2}, L-\frac{1}{2})$ or $(\frac{3}{2}, L+\frac{1}{2})$ channels than for $(\frac{1}{2}, L+\frac{1}{2})$ or $(\frac{3}{2}, L-\frac{1}{2})$. This pattern is even more pronounced if, for each L, one considers energies ranging up the 'natural' scale characterizing the resonance region of that partial wave (a precise determination of these 'natural' scales is unimportant). Certainly in a case such as this a picture is worth a thousand words; we present the relevant pictures in Fig. 4. (Not surprisingly, the only exception to the rule is in the recalcitrant D_{35} channel; also, the G_{19} amplitude is as large as the G_{39}.)

Clearly, this pattern of size alternation is consistent with Eqs. (3.22a) and (3.22b), since, in these equations, the $(\frac{3}{2}, L-\frac{1}{2})$ and $(\frac{3}{2}, L+\frac{1}{2})$ amplitudes are linked by large coefficients to the $(\frac{1}{2}, L+\frac{1}{2})$ and $(\frac{1}{2}, L-\frac{1}{2})$ amplitudes, respectively. But of course, the reversed pattern, with the 'small' and 'large' channels interchanged, would have been equally consistent. For a more compelling argument, one must necessarily go beyond the purely group-theoretic reasoning that led to (3.22) and add a single plausible dynamical assumption.

To this end, let us return to Eq. (3.15), in which the physical $\pi N \to \pi N$ amplitudes in the Lth partial wave are expressed as linear combinations of the 'reduced' amplitudes $\mathbf{s}_{KLL}$ with $K = L-1, L, L+1$. Now, in the specific case of the Skyrme model, it turns out that the variation of $\mathbf{s}_{L+1,LL}$ away from unity is essentially negligible compared to that of $\mathbf{s}_{L-1,LL}$ and $\mathbf{s}_{LLL}$ for energies less than 2.5 MeV, as discussed in Ref. 7. Certainly it is not unreasonable to assume that this continues to be true for the 'optimal' two-flavor effective Lagrangian, especially in light of the relatively high degree of success with which the Skyrme model is able to reproduce the full spectrum of nucleon and delta resonances in

Nature[6,7] . If accordingly we make the dynamical assumption that $s_{L+1,LL} \approx 1$ throughout the relevant energy ranges (ignoring inelasticities for the sake of simplicity) and represent the physical amplitude $S_{LL\frac{1}{2}\frac{1}{2}IJ}$ more compactly as S_{LIJ}, then Eq. (3.15) becomes:

$$\begin{aligned}
S_{L\frac{1}{2},L-\frac{1}{2}} - 1 &= \frac{2L-1}{3L} \cdot (s_{L-1,LL} - 1) + \frac{L+1}{3L} \cdot (s_{LLL} - 1), \\
S_{L\frac{1}{2},L+\frac{1}{2}} - 1 &= \frac{L}{3L+3} \cdot (s_{LLL} - 1), \\
S_{L\frac{3}{2},L-\frac{1}{2}} - 1 &= \frac{(2L-1)(L-1)}{6L(2L+1)} \cdot (s_{L-1,LL} - 1) + \frac{2L-1}{6L} \cdot (s_{LLL} - 1), \\
S_{L\frac{3}{2},L+\frac{1}{2}} - 1 &= \frac{2L-1}{4L+2} \cdot (s_{L-1,LL} - 1) + \frac{2L+3}{6L+6} \cdot (s_{LLL} - 1).
\end{aligned} \tag{4.3}$$

The pattern of alternating size now emerges as an automatic consequence of the group theory: it is simply due to the relatively small coefficients in the middle two equations of (4.3) as compared to the outer two. A further prediction of these expressions is that, of the two 'large' amplitudes, $S_{L\frac{1}{2},L-\frac{1}{2}}$ should dominate $S_{L\frac{3}{2},L+\frac{1}{2}}$—and, with the single exception of the P-channels, this is also apparent in Fig. 4.

5. Comparison with Experiment: $\pi N \to \pi\Delta$

We conclude with a brief examination of the inelastic process $\pi N \to \pi\Delta$ in the chiral soliton framework. We should remark at the outset that this process constitutes a much more tenuous proving ground for the chiral soliton ansatz than the elastic case: On the one hand, the extraction of partial-wave amplitudes from experiment requires a nontrivial and model-dependent analysis to disentangle $\pi\Delta$ from a variety of other final states such as ρN, ϵN and πN^*. On the other hand,

from a theoretical point of view, several of the approximations we have invoked in the derivation of the linear relations become substantially more drastic in the inelastic case, as we have discussed in Section 2. Throughout this section we draw from the recent partial-wave analysis of Manley *et al.*[9] ; the $\pi\Delta$ data presented there is restricted to $W \leq 2$ GeV and $L \leq 3$[#6]

We begin by looking at processes in which the pion jumps two units of angular momentum. From Eq. (3.24) we predict simple proportionality relations between partial-wave amplitudes[#7] :

$$SD_{11} = -\sqrt{2} \cdot DS_{13} = -\sqrt{10} \cdot SD_{31} = \sqrt{20} \cdot DS_{33} \qquad (5.1a)$$

and

$$FP_{15} = -\sqrt{10} \cdot FP_{35}. \qquad (5.1b)$$

These relations are checked in Fig. 5. For the SD and DS waves, the agreement is not impressive. The relative signs of the four amplitudes are predicted correctly, but there is no evidence for the factor of $\sqrt{10}$ which connects the first and second pairs of terms in Eq. (5.1*a*). One should note, of course, that these channels all couple to the translation zero-modes. For the FP waves, which do not, the agreement is quite satisfactory, up to the customary 150-200 MeV energy shift between the isospin-$\frac{1}{2}$ and the isospin-$\frac{3}{2}$ amplitudes.

#6 The analysis of ref. 9 presents the values of the partial-wave amplitudes derived from an energy-independent analysis and a unitary, energy-dependent fit to this values. Because the directly extracted amplitudes are often sparse and erratic, we have chosen to use the fit in making our comparison. This fit is generally a good representation of the elementary data, but one should note that there are some large deviations, for example, in the SD_{31} and PP_{33} partial waves.

#7 The notation is $LL'_{2I,2J}$, with L and L' the incoming and outgoing pion angular momenta, respectively.

We turn next to processes for which the initial and final pion angular momenta are equal. In both the D- and F-waves, the partial-wave amplitudes for three out of the four possible channels could be resolved from the data in the analysis of Ref. 9. These triplets of amplitudes are predicted to obey the relations:

$$DD_{33} = \frac{4}{5\sqrt{10}} \cdot DD_{13} + \frac{9}{10}\sqrt{\frac{7}{5}} \cdot DD_{15} \tag{5.2a}$$

and

$$FF_{37} = \frac{7}{6\sqrt{6}} \cdot FF_{15} + \frac{2}{3}\sqrt{\frac{5}{3}} \cdot FF_{35}. \tag{5.2b}$$

In Fig. 6 we have displayed the experimental DD_{33} and FF_{37} amplitudes (indicated by solid lines) juxtaposed with the appropriate linear combinations dictated by (5.2) (dotted lines). Although in the first instance (where again there is mixing with the translational mode) the shape of the Argand plot is reasonably rendered, the predicted curve is obviously too big by roughly a factor of four. In the second case, however, as for F-waves in general, the agreement is quite respectable.

Unfortunately, out of the four possible PP processes, only PP_{11} and PP_{33} were considered by Manley, *et al.*, to be adequately determined by the data. This makes it impossible for us to test the validity of Eq. (3.23) for this case. If, however, we assume the PP_{13} amplitude to be small, Eq. (3.23*b*) suggests that the PP_{11} and PP_{33} amplitudes will have the same sign; this is indeed what is observed experimentally.

We turn, finally, to Eq. (3.25), which links the processes $\pi N \to \pi N$ and $\pi N \to \pi\Delta$. The relations which follow from (3.25) may be expressed in several

different ways, by combining this equation with the relations (3.22) and (3.23) already discussed. For example, one may obtain:

$$\frac{1}{\sqrt{2}}(P_{11} - P_{13}) = \frac{5}{4} \cdot PP_{33} - \frac{1}{8} \cdot PP_{11}; \qquad (5.3a)$$

$$\frac{1}{\sqrt{2}}(D_{13} - D_{33}) = \frac{9}{10\sqrt{2}} \cdot DD_{13} + \frac{9\sqrt{7}}{20} \cdot DD_{15}; \qquad (5.3b)$$

$$\frac{1}{\sqrt{2}}(F_{15} - F_{17}) = \frac{1}{2} \cdot FF_{35} + \sqrt{\frac{3}{5}} \cdot FF_{37}. \qquad (5.3c)$$

The left- and right-hand sides of these equations are compared in Fig. 7; they are indicated by solid and dotted lines, respectively. The comparisons are typical among the choices which we have examined, though different choices yield curves of very different size[♯8] . In making this comparison, it is also necessary to choose a convention for relating energies in $\pi N \to \pi\Delta$ to those in $\pi N \to \pi N$. It is not clear to us to us whether it is best to define the excitation energy in $\pi N \to \pi\Delta$ as starting from the πN or the $\pi\Delta$ threshold; as a compromise we have taken the average of the two (for these graphs only). Once again, although the sizes of the amplitudes are not in especially close agreement, the signs are correctly given and the general shapes are similar.

All in all, we can conclude that the limited $\pi N \to \pi\Delta$ data, while not particularly compelling in and of itself, is certainly consistent with the elegant interpretation of the baryon as a soliton in the field of pions.

♯8 We should note, though, that in (5.3) we have avoided combinations which require cancelations among large amplitudes, or which involve the exceptional channels P_{33} and D_{35}.

ACKNOWLEDGMENTS

We have greatly benefited from discussions with Marek Karliner, Fred Gilman and David Leith, and we are indebted to Richard Arndt and G. Höhler for helpful correspondence concerning their data compilations. M. M. would especially like to thank Judy Hochberg for several months' gentle forbearance. Finally, we are grateful to James Voisinet for salvaging Section 3.

APPENDIX A: Derivation of Eq. (3.14)

The purpose of this appendix is to fill in the steps between Eqs. (3.12) and (3.13). We shall not assume isospin and angular momentum conservation *ab initio*; these will emerge in the course of our derivation.

We begin by considering the integral over the $SU(2)$ group manifold in (3.12). Changing variables to $A\epsilon^{-1}$ transforms the integral to

$$\begin{aligned}\int dA\, A_{(R')i'_s s'_s} \left(A_{(1)}\epsilon_{(1)}\right)_{im} \left(\epsilon^{-1}_{(1)}A^{-1}_{(1)}\right)_{nj} \left(A^{-1}_{(R)}\right)_{s_s i_s} \\ = (-1)^{n-m} \int dA\, A_{(R')i'_s s'_s} A_{(1)i,-m} (A_{(1)}{}^{-1})_{-n,j} (A^{-1}_{(R)})_{s_s i_s}\end{aligned} \tag{A.1}$$

using

$$\epsilon_{(1)} = \begin{pmatrix} 0 & 0 & 1 \\ 0 & -1 & 0 \\ 1 & 0 & 0 \end{pmatrix} .$$

It turns out that the A-integration can be carried out explicitly, thanks to the Clebsch-Gordon decomposition

$$A_{(R_1)ab} A_{(R_2)cd} = \sum_{\widetilde{R}} A_{(\widetilde{R})a+c,b+d} \left\langle R_1 R_2 ac | \widetilde{R}, a+c \right\rangle \left\langle \widetilde{R}, b+d | R_1 R_2 bd \right\rangle \tag{A.2}$$

and the orthogonality relation

$$\int dA\, A_{(R_1)ab}\left(A^{-1}_{(R_2)}\right)_{cd} = \frac{2\pi^2}{2R_1+1}\,\delta_{R_1R_2}\delta_{bc}\delta_{ad}. \tag{A.3}$$

We obtain:

$$\begin{aligned}\left\langle \pi^i\pi^j\right\rangle_{Ri_zs_z;R'i'_zs'_z} = &\sum_{mn\widetilde{R}} \langle \pi^m\pi^n\rangle_\circ\,(-1)^{n-m}\frac{\sqrt{(2R+1)(2R'+1)}}{2I+1}\\ &\times\left\langle R'1i'_zi|\widetilde{R},j+i_z\right\rangle\left\langle \widetilde{R},s_z-n|R'1s'_z,-m\right\rangle\\ &\times\left\langle R1s_z,-n|\widetilde{R},s_z-n\right\rangle\left\langle \widetilde{R},j+i_z|R1i_zj\right\rangle\end{aligned} \tag{A.4}$$

It is useful to project the initial and final pion-baryon states onto states of definite total isospin $|II_z\rangle$ and $|I'I'_z\rangle$, respectively. A straightforward calculation yields the somewhat simpler expression

$$\begin{aligned}\langle\pi\pi\rangle_{R\vec{I}s_z;R'\vec{I}'s'_z} = &\,\delta_{II'}\delta_{I_zI'_z}\frac{\sqrt{(2R+1)(2R'+1)}}{2I+1}\\ &\times\sum_{mn}(-1)^{n-m}\langle\pi^m\pi^n\rangle_\circ\\ &\times\left\langle I,s_z-n|R'1s'_z,-m\right\rangle\left\langle R1s_z,-n|I,s_z-n\right\rangle\ .\end{aligned} \tag{A.5}$$

Happily, isospin conservation is now manifest in the Kronecker-deltas.

We have not yet arrived at our final destination, where the initial and final pion-baryon states are characterized, not only by definite isospin, but by definite angular momentum as well. But in order to make progress we must necessarily return to the question of diagonalizing the differential operators $\widehat{\mathbf{L}}_{ij}$ defined in Eqs. (3.7) and (3.8). Complicated though $\widehat{\mathbf{L}}$ may be, it respects the symmetry $\vec{K} \equiv \vec{I}(pion) + \vec{L}(pion)$. Consequently $\widehat{\mathbf{L}}$ preserves the subspaces of states of definite K and K_z.

How do we construct these subspaces? Consider the quantity

$$\mathbf{\Pi}_L^{KK_z}(\Omega) = \begin{pmatrix} \langle L1K_z-1,1|KK_z\rangle\ Y_{L,K_z-1}(\Omega) \\ \langle L1K_z0|KK_z\rangle\ Y_{LK_z}(\Omega) \\ \langle L1K_z+1,-1|KK_z\rangle\ Y_{L,K_z+1}(\Omega) \end{pmatrix}; \qquad (A.6)$$

these are the vector spherical harmonics. By the familiar rules for addition of angular momenta $\mathbf{\Pi}_L^{KK_z}$ is indeed a state of definite K and K_z. Unfortunately it also has definite orbital angular momentum L, which is *not* preserved by $\widehat{\mathbf{L}}$: the pion can jump two units in L in the process $\pi N \to \pi\Delta$, for example, in a manner consistent with angular momentum conservation. Therefore, in order to block-diagonalize $\widehat{\mathbf{L}}$ we must sum over all allowed values of L for each K, namely $L = (K-1, K, K+1)$. Parity precludes the states with $L = K$ from mixing with those with $L = K \pm 1$; consequently the eigenstates of $\widehat{\mathbf{L}}$ are of the following form:

$$\text{Parity } (-1)^{L-1}: \quad \psi_-^K(r,t)\mathbf{\Pi}_{K-1}^{KK_z}(\Omega) + \psi_+^K(r,t)\mathbf{\Pi}_{K+1}^{KK_z}(\Omega)$$

$$\text{Parity } (-1)^{L}: \quad \psi_\circ^K(r,t)\mathbf{\Pi}_{K}^{KK_z}(\Omega)\ .$$

One can imagine expanding an arbitrary pion field in terms of these eigenfunctions and carrying out the angular integration in (3.7). The result will be a purely radial problem, where for each value of K, $\widehat{\mathbf{L}}$ is replaced by an operator

$$\widehat{\mathbf{L}}_K^{\text{eff}}(r,t) = \begin{pmatrix} \widehat{\mathbf{L}}_K^{--} & 0 & \widehat{\mathbf{L}}_K^{-+} \\ 0 & \widehat{\mathbf{L}}_K^{\circ\circ} & 0 \\ \widehat{\mathbf{L}}_K^{+-} & 0 & \widehat{\mathbf{L}}_K^{++} \end{pmatrix} \qquad (A.7)$$

acting on the space

$$\begin{pmatrix} \psi_-^K \\ \psi_\circ^K \\ \psi_+^K \end{pmatrix}$$

with the zeroes of course reflecting parity conservation.

Furthermore from the radial wavefunctions $\psi^K(r,t)$ one can construct the "effective" Green's functions $\mathbf{g}_K(rt;r't')$ associated with $\hat{\mathbf{L}}_K^{\text{eff}}$; this is of course a 3×3 matrix checkered with zeroes just as in (A.7). We will find it convenient to label its matrix elements by pairs of subscripts (L,L') that take values $(K-1, K, K+1)$ instead of the usual (1,2,3) or $(+,0,-)$; thus $\mathbf{g}_{435}$, say, instead of $(\mathbf{g}_4)_{1,3}$.

Having defined $\mathbf{g}_K$ we are now in a position to write down the partial wave decomposition of the pion propagator in the unrotated soliton background. One finds

$$\begin{aligned}\left\langle \pi^m(\vec{x}'t')\pi^{n*}(\vec{x},t)\right\rangle_\circ = \sum_{LL_zL'L'_z} \Big\{ & Y_{L'L'_z}(\Omega')Y^*_{LL_z}(\Omega)\times \\ & \sum_{KK_z} \langle KK_z|L1L_zn\rangle \left\langle L'1L'_zm|KK_z\right\rangle \mathbf{g}_{KL'L}(rt;r't')\Big\}\end{aligned} \tag{A.8}$$

with $\vec{L}$ and $\vec{L}'$ the incoming and outgoing pion angular momentum, respectively. This formula will presently prove very useful to us.

We now have all the machinery in place for our final result. We return to Eq. (A.5) and project the initial and final pion-baryon states onto states of definite total angular momentum $|JJ_z\rangle$ and $|J'J'_z\rangle$, respectively; likewise the incoming and outgoing pions are restricted to partial waves L and L', which we still have the freedom to specify. A short calculation making use of (A.8) then produces

$$\langle\pi\pi\rangle_{R\bar{I}\bar{J}L;R'\bar{I}'\bar{J}'L'} = \delta_{II'}\delta_{I_zI_z'}\frac{\sqrt{(2R+1)(2R'+1)}}{2I+1}$$
$$\times \sum_{KK_zmn}\sum_{s_zs_z'L_zL_z'}(-1)^{n-m}g_{KL'L}$$
$$\times \langle RLs_zL_z|JJ_z\rangle\ \langle J'J_z'|R'L's_z'L_z'\rangle \qquad (A.9)$$
$$\times \langle I, s_z-n|R'1s_z', -m\rangle\ \langle R1s_z, -n|I, s_z-n\rangle$$
$$\times \langle KK_z|L1L_zn\rangle\ \langle L'1L_z'm|KK_z\rangle\ .$$

It is certainly not manifest from this rather unwieldy formula that total angular momentum is conserved, as of course it must be. In order to see that, it is convenient to reexpress the Clebsch-Gordon coefficients as $3j$-symbols

$$\begin{pmatrix} j_1 & j_2 & J \\ m_1 & m_2 & -M \end{pmatrix} = (-1)^{j_1-j_2+M}(2J+1)^{-1/2}\langle j_1j_2m_1m_2|JM\rangle\ .$$

These, in turn, can be used to construct the $6j$-symbols via

$$\sum_{M_1M_2M_3}(-1)^{J_1+J_2+J_3+M_1+M_2+M_3}\begin{pmatrix} J_1 & J_2 & j_3 \\ M_1 & -M_2 & m_3 \end{pmatrix}$$
$$\times\begin{pmatrix} J_2 & J_3 & j_1 \\ M_2 & -M_3 & m_1 \end{pmatrix}\begin{pmatrix} J_3 & J_1 & j_2 \\ M_3 & -M_1 & m_2 \end{pmatrix}$$
$$=\begin{pmatrix} j_1 & j_2 & j_3 \\ m_1 & m_2 & m_3 \end{pmatrix}\begin{Bmatrix} j_1 & j_2 & j_3 \\ J_1 & J_2 & J_3 \end{Bmatrix}$$

A short calculation making use of some standard properties of $6j$-symbols produces

$$\langle\pi(r't')\pi(rt)\rangle_{R\bar{I}\bar{J}L;R'\bar{I}'\bar{J}'L'}$$
$$= \delta_{II'}\delta_{I_zI_z'}\delta_{JJ'}\delta_{J_zJ_z'}\sum_K P_{LL'RR'IJK}\cdot g_{KL'L}(rt;r't') \qquad (A.10)$$

where the P-symbols are defined in Eq. (3.14). Both isospin and angular momentum are now manifestly conserved. This is Eq. (3.13).

APPENDIX B: Explicit formulae for P-symbols

This appendix contains explicit formulas for those P-symbols as defined by Eq. (3.14) which contribute to either $\pi N \to \pi N$ or $\pi N \to \pi \Delta$. The notation is $P_{LL'RR'IJK}$ where L and L' give the orbital angular momentum of the incoming and outgoing pion, respectively; R and R' denote the spin (and isospin) representation of the initial and final baryon; I and J are total isospin and angular momentum; and K labels the conserved vector $\vec{I}(pion) + \vec{L}(pion)$.

We consider first the process $\pi N \to \pi N$, which in our notation implies $L = L'$ and $R = R' = \frac{1}{2}$. With two exceptions as noted below, the scattering must be P-wave or higher in order for the P-symbol not to vanish. For $L \geq 1$ the nonvanishing values of the P-symbols are given by:

$$
\begin{aligned}
P_{LL\frac{1}{2}\frac{1}{2}\frac{1}{2},L-\frac{1}{2},L-1} &= \frac{2L-1}{3L} \\
P_{LL\frac{1}{2}\frac{1}{2}\frac{1}{2},L-\frac{1}{2},L} &= \frac{L+1}{3L} \\
P_{LL\frac{1}{2}\frac{1}{2}\frac{1}{2},L+\frac{1}{2},L} &= \frac{L}{3L+3} \\
P_{LL\frac{1}{2}\frac{1}{2}\frac{1}{2},L+\frac{1}{2},L+1} &= \frac{2L+3}{3L+3} \quad \text{(also valid for } L=0\text{)} \\
P_{LL\frac{1}{2}\frac{1}{2}\frac{3}{2},L-\frac{1}{2},L-1} &= \frac{(2L-1)(L-1)}{6L(2L+1)} \\
P_{LL\frac{1}{2}\frac{1}{2}\frac{3}{2},L-\frac{1}{2},L} &= \frac{2L-1}{6L} \\
P_{LL\frac{1}{2}\frac{1}{2}\frac{3}{2},L-\frac{1}{2},L+1} &= \frac{2L+3}{4L+2} \\
P_{LL\frac{1}{2}\frac{1}{2}\frac{3}{2},L+\frac{1}{2},L-1} &= \frac{2L-1}{4L+2} \\
P_{LL\frac{1}{2}\frac{1}{2}\frac{3}{2},L+\frac{1}{2},L} &= \frac{2L+3}{6L+6} \\
P_{LL\frac{1}{2}\frac{1}{2}\frac{3}{2},L+\frac{1}{2},L+1} &= \frac{(L+2)(2L+3)}{(6L+6)(2L+1)} \quad \text{(also valid for } L=0\text{)} \ .
\end{aligned}
\tag{B.1}
$$

Consider, next, the process $\pi N \to \pi\Delta$ with $L = L'$. Here L must be ≥ 1 without exception, in which case the nonvanishing P-symbols are:

$$
\begin{aligned}
P_{LL\frac{1}{2}\frac{3}{2}\frac{1}{2},L-\frac{1}{2},L-1} &= \frac{\sqrt{(L+1)(2L-1)}}{3L} \\
P_{LL\frac{1}{2}\frac{3}{2}\frac{1}{2},L-\frac{1}{2},L} &= \frac{-\sqrt{(L+1)(2L-1)}}{3L} \\
P_{LL\frac{1}{2}\frac{3}{2}\frac{1}{2},L+\frac{1}{2},L} &= \frac{\sqrt{L(2L+3)}}{3L+3} \\
P_{LL\frac{1}{2}\frac{3}{2}\frac{1}{2},L+\frac{1}{2},L+1} &= \frac{-\sqrt{L(2L+3)}}{3L+3} \\
P_{LL\frac{1}{2}\frac{3}{2}\frac{3}{2},L-\frac{1}{2},L-1} &= \frac{4(L-1)}{3L(2L+1)}\sqrt{\frac{(2L-1)(L+1)}{10}} \\
P_{LL\frac{1}{2}\frac{3}{2}\frac{3}{2},L-\frac{1}{2},L} &= \frac{(L+4)}{3L}\sqrt{\frac{2L-1}{10(L+1)}} \\
P_{LL\frac{1}{2}\frac{3}{2}\frac{3}{2},L-\frac{1}{2},L+1} &= -\frac{2L+3}{2L+1}\sqrt{\frac{2L-1}{10(L+1)}} \\
P_{LL\frac{1}{2}\frac{3}{2}\frac{3}{2},L+\frac{1}{2},L-1} &= \frac{(2L-1)}{2L+1}\sqrt{\frac{2L+3}{10L}} \\
P_{LL\frac{1}{2}\frac{3}{2}\frac{3}{2},L+\frac{1}{2},L} &= -\frac{L-3}{3L+3}\sqrt{\frac{2L+3}{10L}} \\
P_{LL\frac{1}{2}\frac{3}{2}\frac{3}{2},L+\frac{1}{2},L+1} &= -\frac{4(L+2)}{(3L+3)(2L+1)}\sqrt{\frac{L(2L+3)}{10}} \,.
\end{aligned}
\tag{B.2}
$$

The final possibility is $\pi N \to \pi\Delta$ with $L = L' \pm 2$. Now $L = 0$ *is* allowed, and we have:

$$P_{L,L+2,\frac{1}{2}\frac{3}{2}\frac{1}{2},L+\frac{1}{2},L+1} = -\sqrt{\frac{2L+3}{3(L+1)}}$$

$$P_{L,L+2,\frac{1}{2}\frac{3}{2}\frac{3}{2},L+\frac{1}{2},L+1} = \sqrt{\frac{2L+3}{30(L+1)}} \qquad (B.3)$$

$$P_{L+2,L\frac{1}{2}\frac{3}{2}\frac{1}{2},L+\frac{3}{2},L+1} = \sqrt{\frac{2L+3}{3(L+2)}}$$

$$P_{L+2,L\frac{1}{2}\frac{3}{2}\frac{3}{2},L+\frac{3}{2},L+1} = -\sqrt{\frac{2L+3}{30(L+2)}}$$

All other P-symbols with $R = \frac{1}{2}$ and $R' = \frac{1}{2}$ or $\frac{3}{2}$ vanish.

REFERENCES

1. For a review, see S. Gasiorowicz and D. Geffen, *Rev. Mod. Phys.* **41**, 531 (1969).
2. E. Witten, *Nucl. Phys.* **B160**, 57 (1979).
3. E. Witten, *Nucl. Phys.* **B223**, 422 (1983); *ibid.*, 433.
4. G. T. H. Skyrme, *Proc. Roy. Soc.*, **A260**, 127 (1961).
5. D. Finkelstein and J. Rubinstein, *J. Math. Phys.* **9**, 1762 (1968).
6. A. Hayashi, G. Eckart, G. Holzwarth, and H. Walliser, *Phys. Lett.* **147B**, 5 (1984).
7. M. P. Mattis and M. Karliner, SLAC-PUB-3539 (1984).
8. G. Adkins, C. Nappi, and E. Witten, *Nucl. Phys.* **B228**, 552 (1983)
9. D. M. Manley, R. A. Arndt, Y. Goradia, and V. L. Teplitz, *Phys. Rev.* **D30**, 904 (1984).
10. I. Zahed, U.-G. Meissner, and U. B. Kaulfuss, *Nucl. Phys.* **A426**, 525 (1984).
11. A. Hayashi and G. Holzwarth, *Phys. Lett.* **140B**, 175 (1984).
12. J. D. Breit and C. R. Nappi, *Phys. Rev. Lett.* **53**, 889 (1984).
13. H. Walliser and G. Eckart, *Nucl. Phys.* **A429**, 514 (1984).
14. See, for example, J. R. Taylor, *Scattering Theory.* (Wiley, N. Y., 1972).
15. G. Höhler, F. Kaiser, R. Koch, and E. Pietarinen, *Handbook of Pion-Nucleon Scattering* (Fachinformationszentrum, Karlsruhe, 1979), Physik Daten No. 12-7.
16. S. Weinberg, *Phys. Rev. Lett.* **17**, 168 (1966).

17. H. Schnitzer, *Phys. Lett.* **139B**, 217 (1984).

FIGURE CAPTIONS

1. Relation of the six coupled angular momenta in either the initial or the final state of pion-baryon scattering.

2. Experimentally determined $I = \frac{3}{2}$ partial-wave amplitudes for πN elastic scattering, plotted together with the linear combinations of $I = \frac{1}{2}$ amplitudes which should reproduce them if Eq. (3.22) is valid. The $I = \frac{3}{2}$ amplitudes are indicated by solid lines, the $I = \frac{1}{2}$ combinations by dotted lines. We have used the values of these amplitudes presented by Höhler, *et al.*[15] .

3. Speed of motion $|d\mathbf{T}/dW|$ of the *predicted* P_{33} πN elastic scattering amplitude, $P_{33}^{\text{pred}} = \frac{1}{2}P_{11} + \frac{1}{2}P_{13}$. ΔW is the energy above threshold (1077 MeV).

4. Motion of the various πN scattering amplitudes in the unitarity circle, over a range of W from threshold into the resonance region in that channel.

5. $\pi N \to \pi\Delta$ processes in which the pion jumps two units of angular momentum: (a). Test of Eq. (5.1*a*) by comparison of the various SD and DS $\pi N \to \pi\Delta$ partial-wave amplitudes. The upper graph plots SD_{11} against $-\sqrt{2} \cdot DS_{13}$; the lower graph plots SD_{31} against $-\sqrt{2} \cdot DS_{33}$. (b). Test of Eq. (5.1*b*) by comparison of FP_{15} to $-\sqrt{10} \cdot FP_{35}$. In each case, the first-named amplitude is represented by the solid curve. Here and in Figs. 6 and 7, we have used the values of these amplitudes corresponding to the fits presented by Manley, *et al.*[9]

6. $\pi N \to \pi\Delta$ processes in which the initial and final pion angular momenta are equal. The DD_{33} and FF_{37} amplitudes (solid lines) are juxtaposed with

the linear combinations to which they are predicted to correspond via Eq. (5.2) (dotted lines).

7. Comparison of $\pi N \to \pi N$ and $\pi N \to \pi\Delta$ scattering in the same partial wave. The linear combinations of elastic amplitudes (solid lines) are juxtaposed with the appropriate combinations of inelastic amplitudes (dotted lines) as dictated by Eq. (5.3). Excitation energy ΔW is measured from the πN threshold in the elastic case, and from the *average* of the πN and $\pi\Delta$ thresholds in the inelastic case.

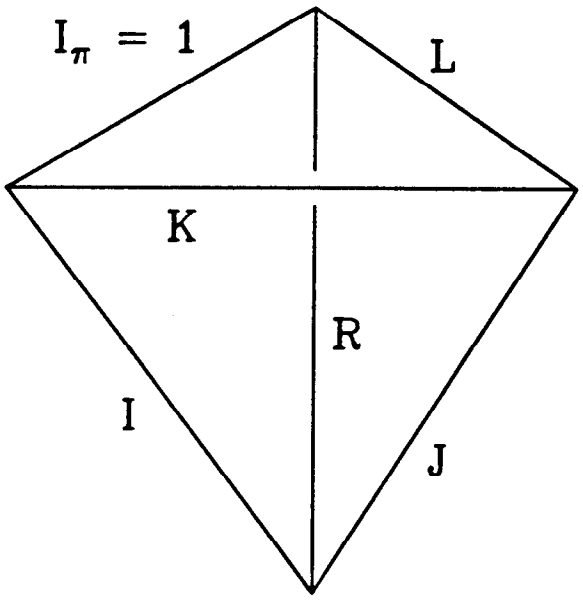

FIG. 1

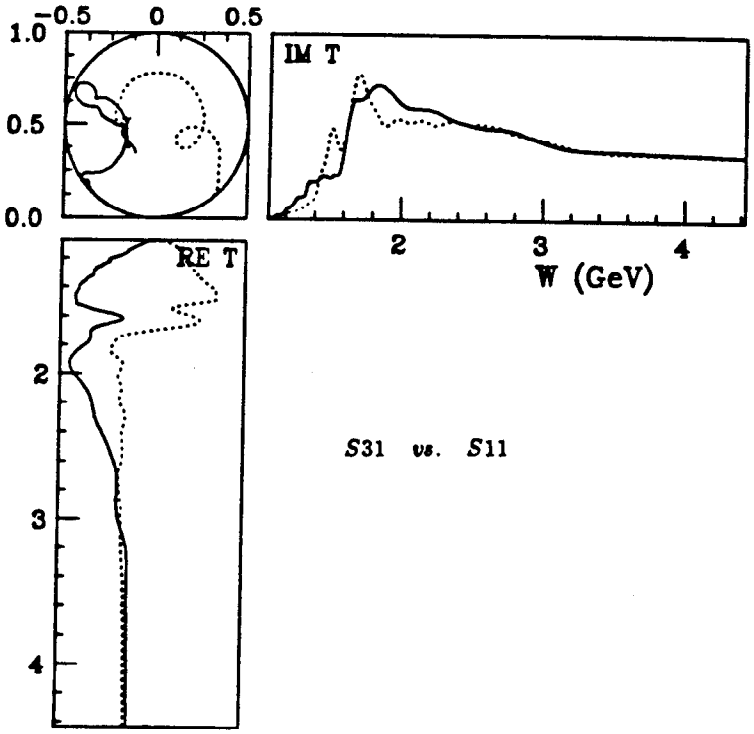

$S31$ *vs.* $S11$

FIG. 2 (page 1)

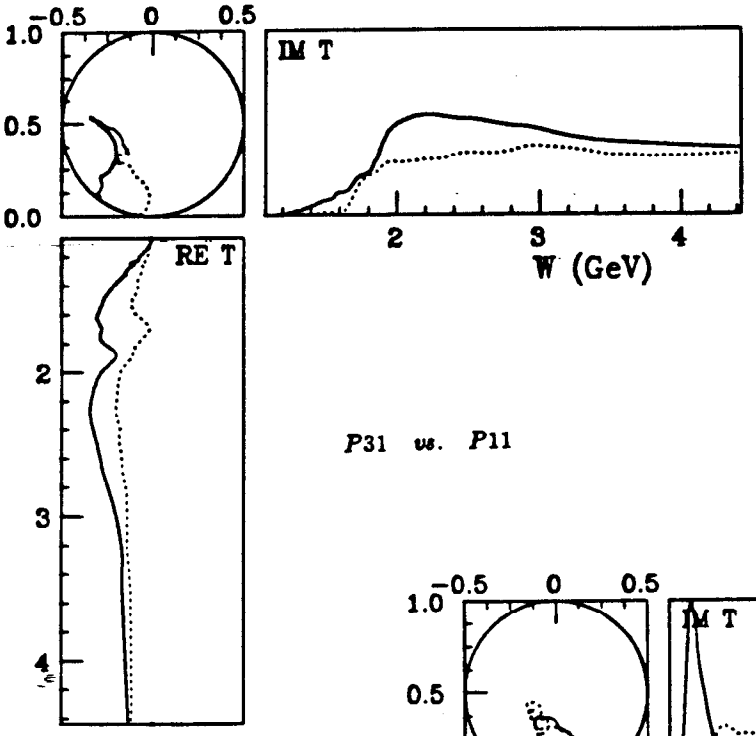

$P31$ *vs.* $P11$

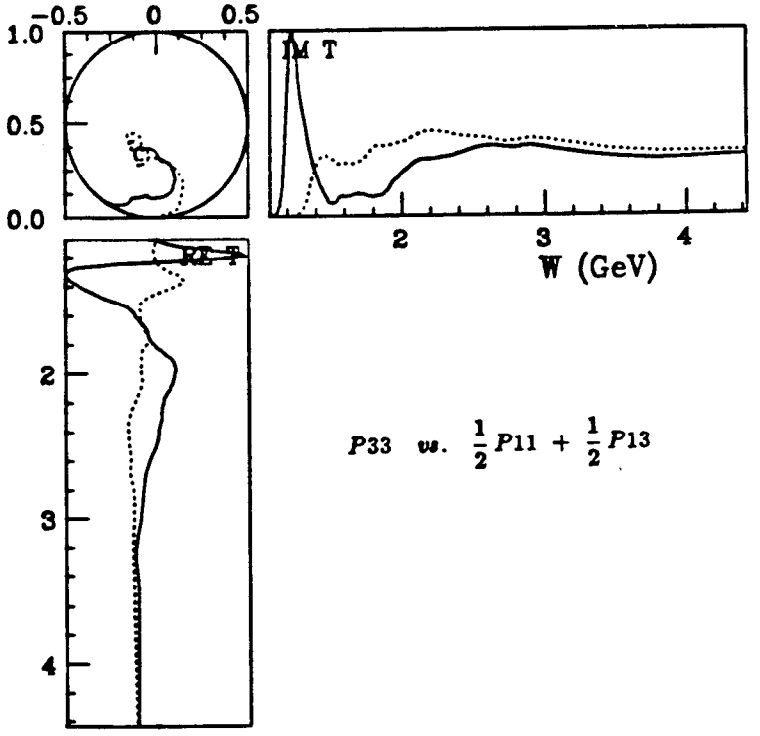

$P33$ *vs.* $\frac{1}{2}P11 + \frac{1}{2}P13$

FIG. 2 (page 2)

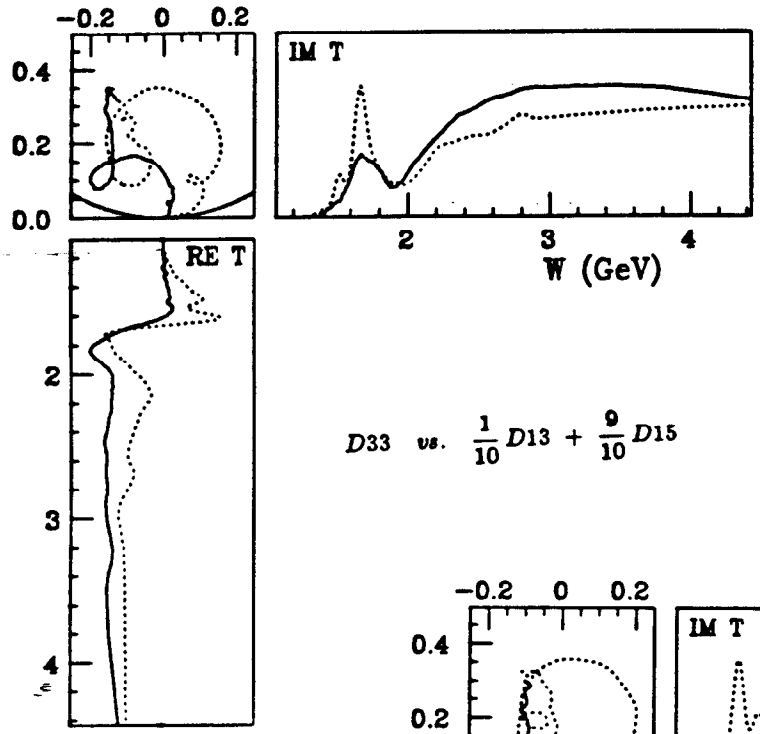

$D33$ *vs.* $\frac{1}{10}D13 + \frac{9}{10}D15$

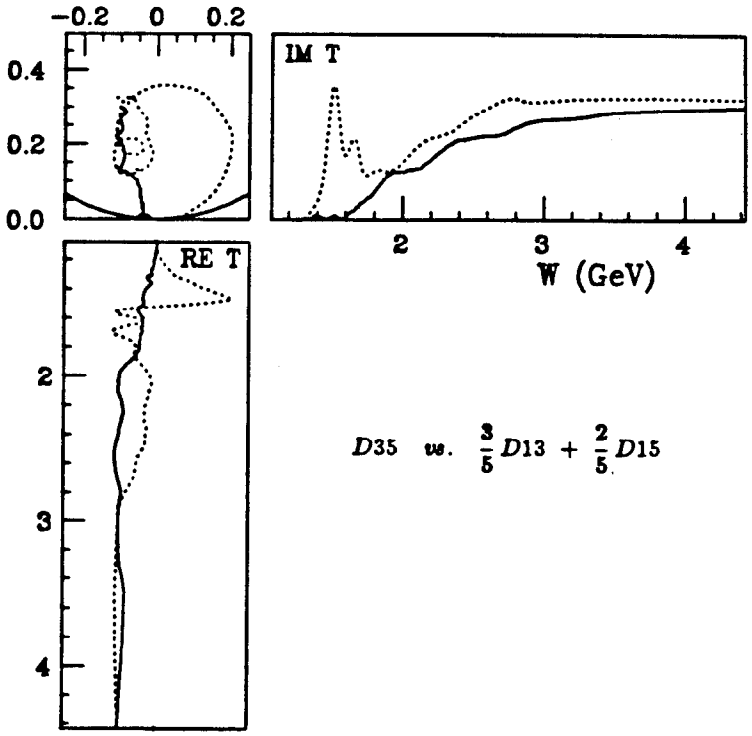

$D35$ *vs.* $\frac{3}{5}D13 + \frac{2}{5}D15$

FIG. 2 (page 3)

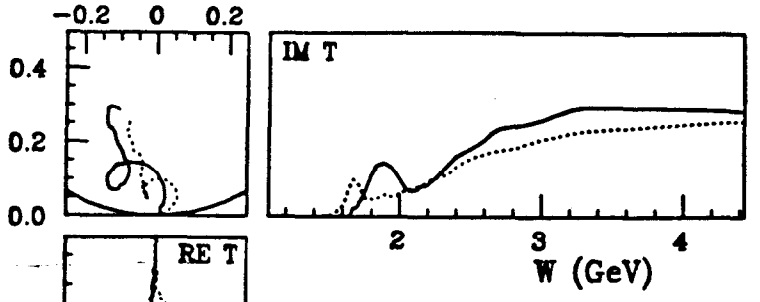

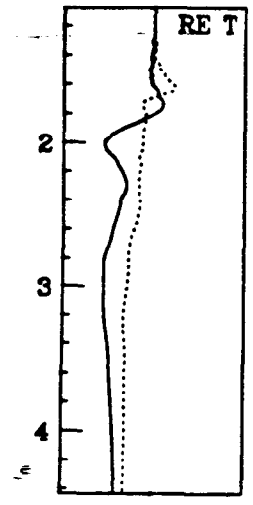

$F35 \quad vs. \quad \frac{1}{7}F15 + \frac{6}{7}F17$

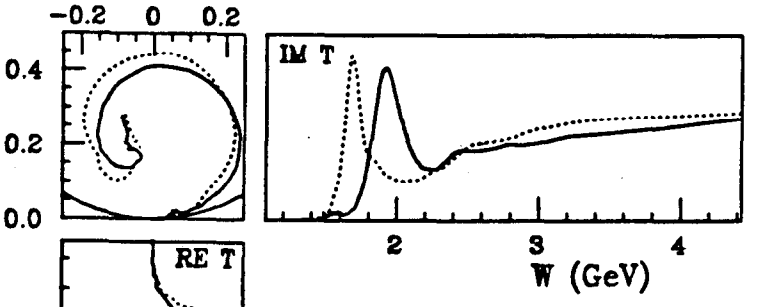

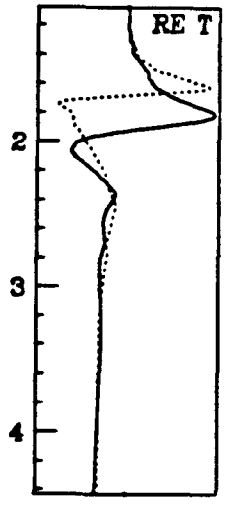

$F37 \quad vs. \quad \frac{9}{14}F15 + \frac{5}{14}F17$

FIG. 2 (page 4)

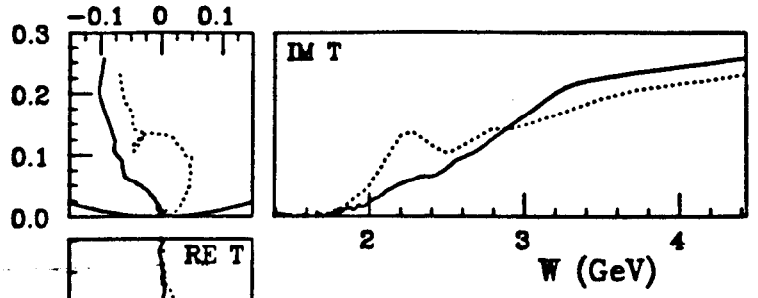

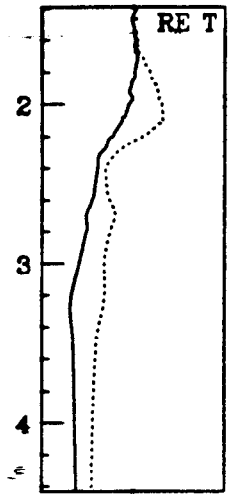

$G37$ *vs.* $\frac{1}{6}G17 + \frac{5}{6}G19$

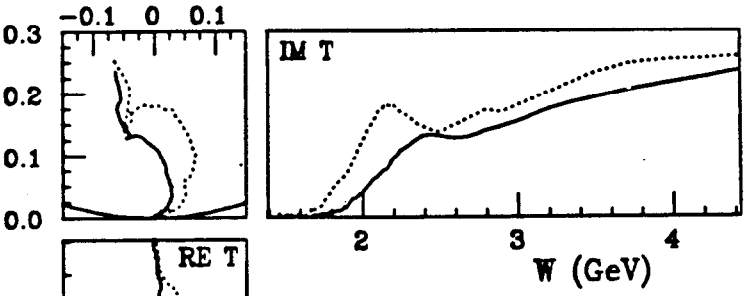

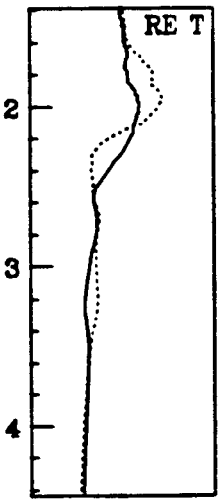

$G39$ *vs.* $\frac{2}{3}G17 + \frac{1}{3}G19$

FIG. 2 (page 5)

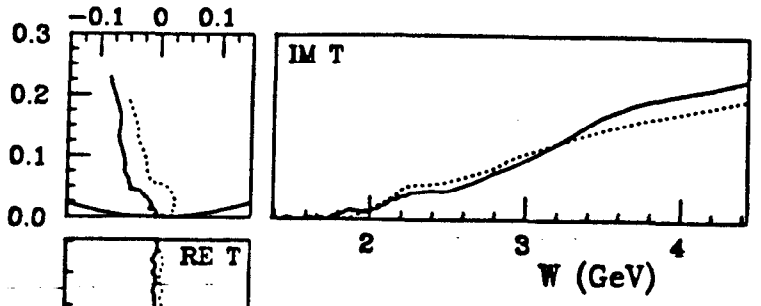

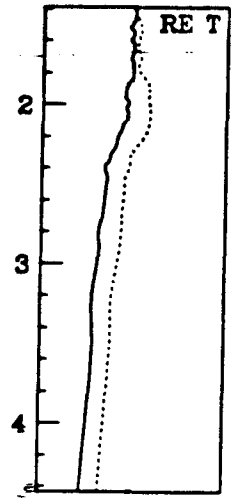

$H39$ *vs.* $\frac{2}{11}H19 + \frac{9}{11}H111$

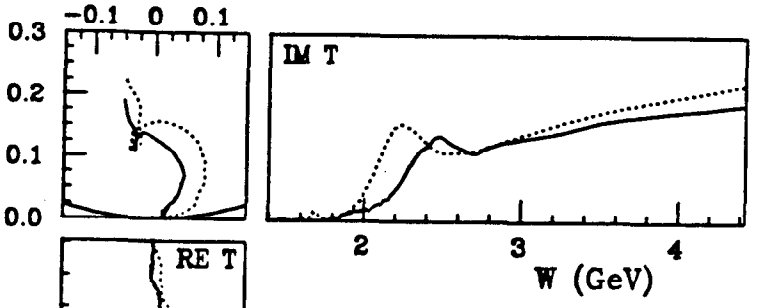

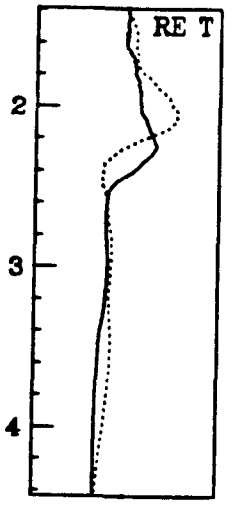

$H311$ *vs.* $\frac{15}{22}H19 + \frac{7}{22}H111$

FIG. 2 (page 6)

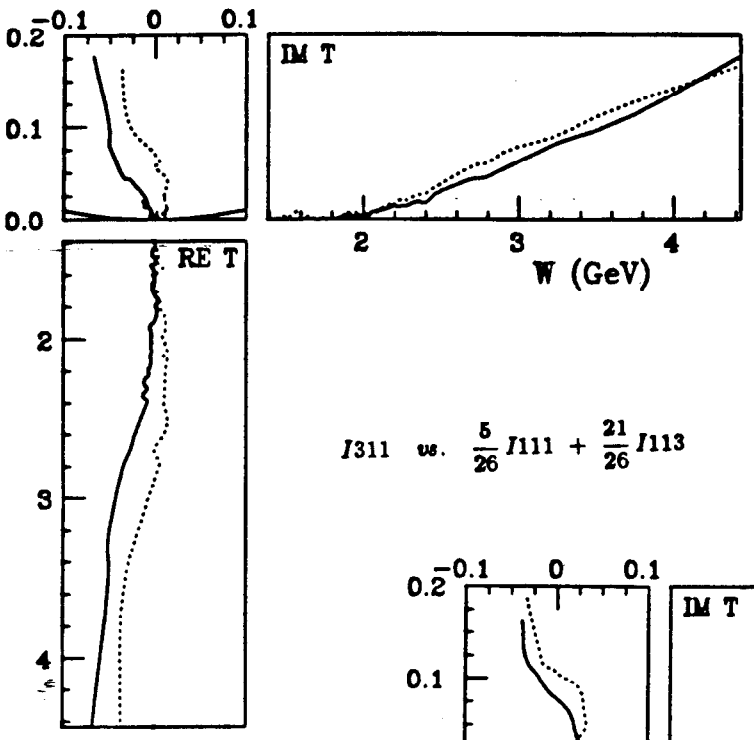

$I311$ *vs.* $\frac{5}{26} I111 + \frac{21}{26} I113$

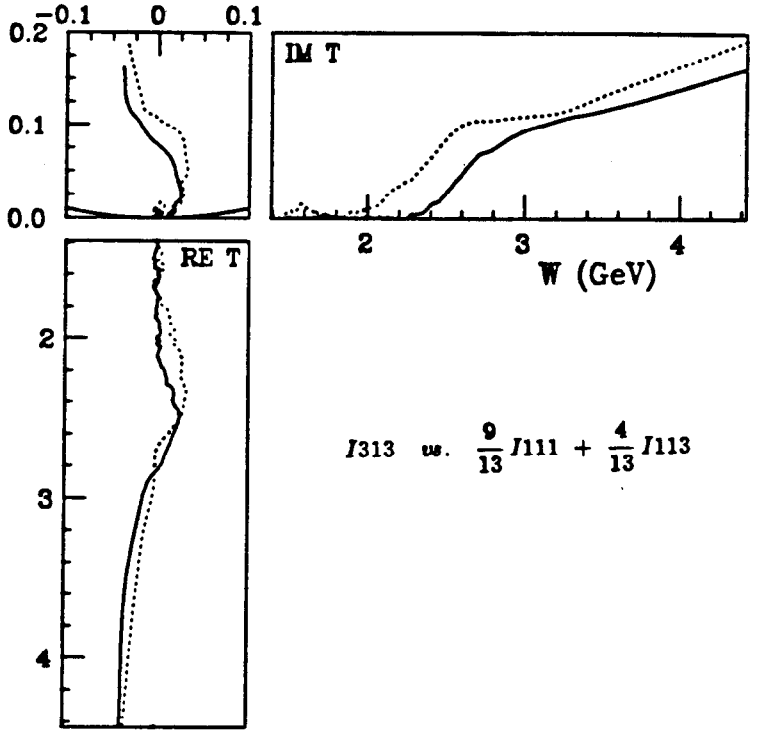

$I313$ *vs.* $\frac{9}{13} I111 + \frac{4}{13} I113$

FIG. 2 (page 7)

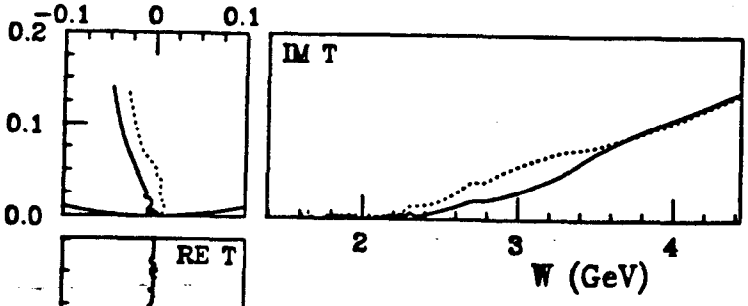

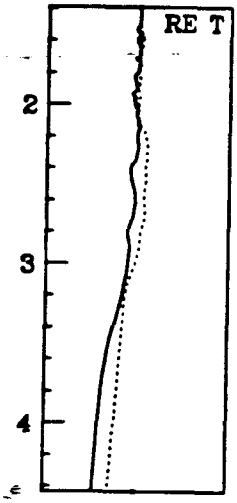

$K313$ *vs.* $\frac{1}{5}K113 + \frac{4}{5}K115$

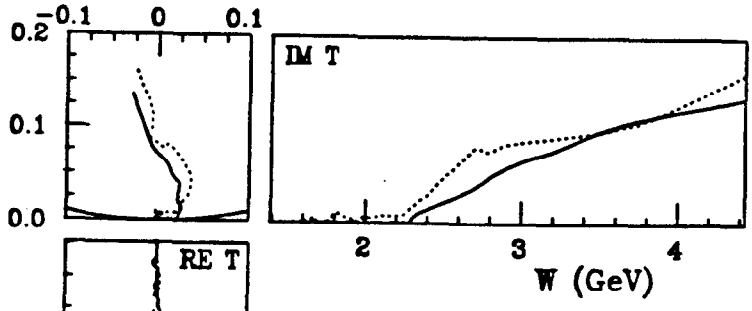

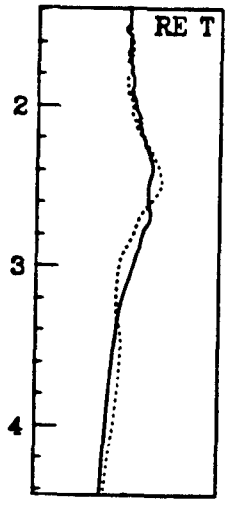

$K315$ *vs.* $\frac{7}{10}K113 + \frac{3}{10}K115$

FIG. 2 (page 8)

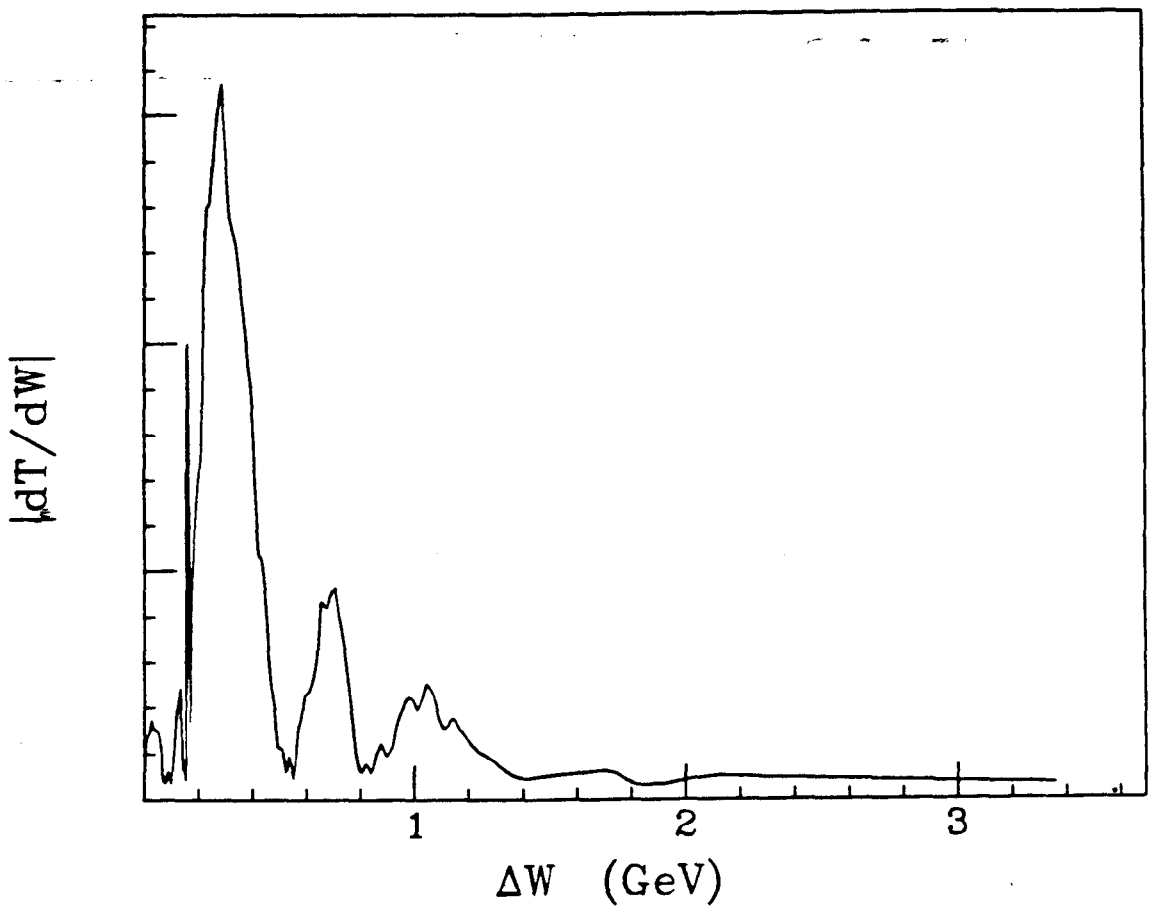

FIG. 3

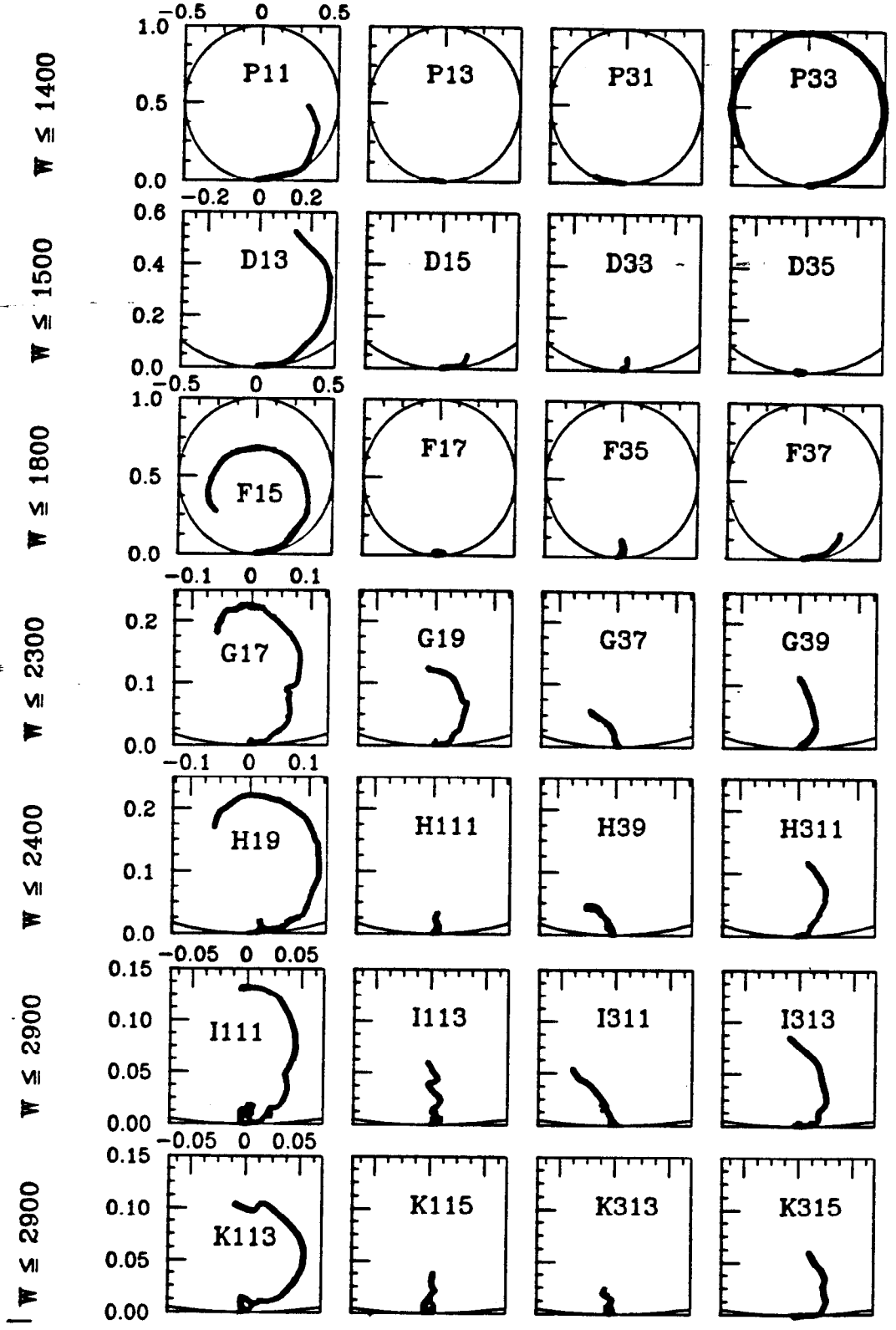
W ≤ 1400
W ≤ 1500
W ≤ 1800
W ≤ 2300
W ≤ 2400
W ≤ 2900
W ≤ 2900
P11
P13
P31
P33
D13
D15
D33
D35
F15
F17
F35
F37
G17
G19
G37
G39
H19
H111
H39
H311
I111
I113
I311
I313
K113
K115
K313
K315

FIG. 4

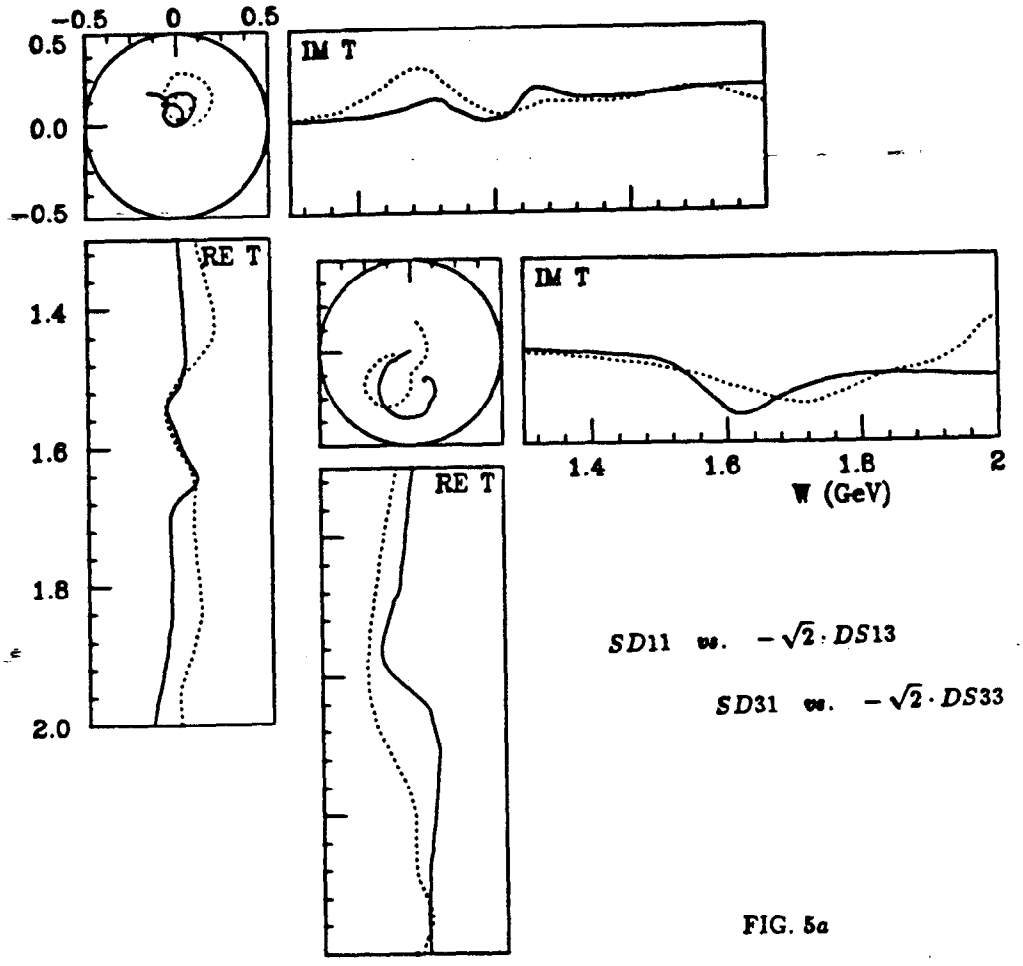

$SD11$ vs. $-\sqrt{2} \cdot DS13$

$SD31$ vs. $-\sqrt{2} \cdot DS33$

FIG. 5*a*

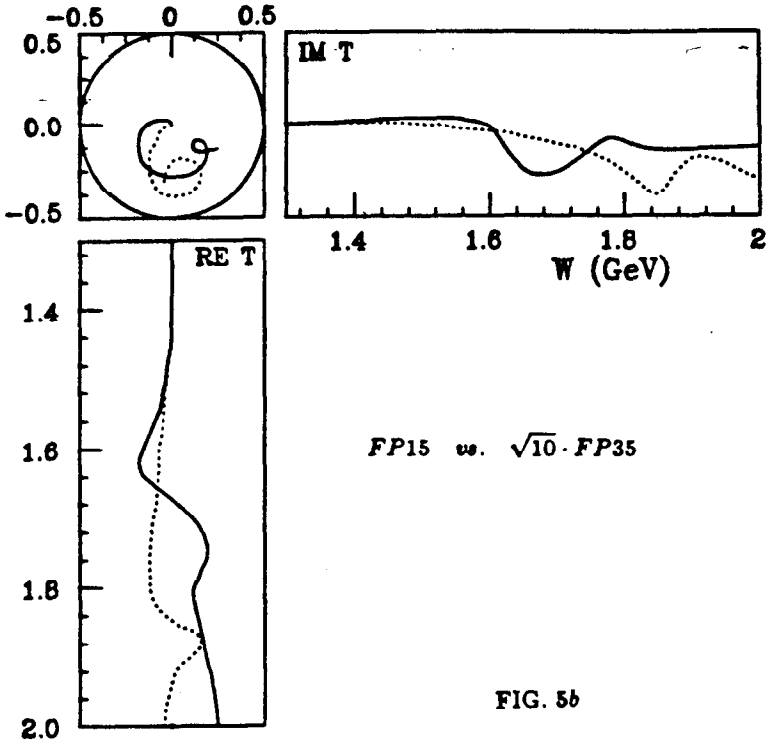

$FP15$ *vs.* $\sqrt{10} \cdot FP35$

FIG. 5*b*

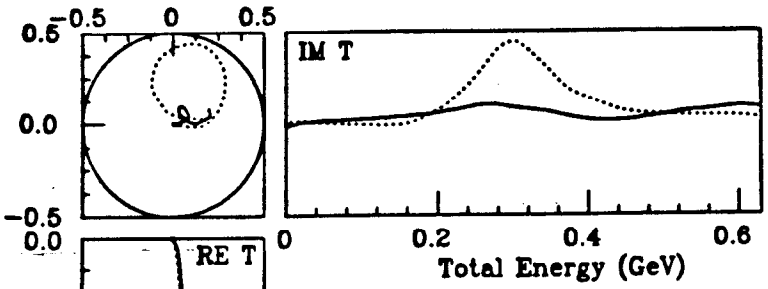

FIG. 6a

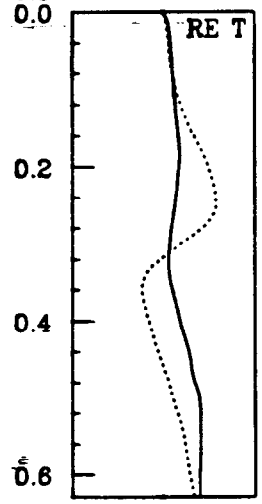

$$DD33 \quad vs. \quad \frac{4}{5\sqrt{10}} \cdot DD13 + \frac{9}{10}\sqrt{\frac{7}{5}} \cdot DD15$$

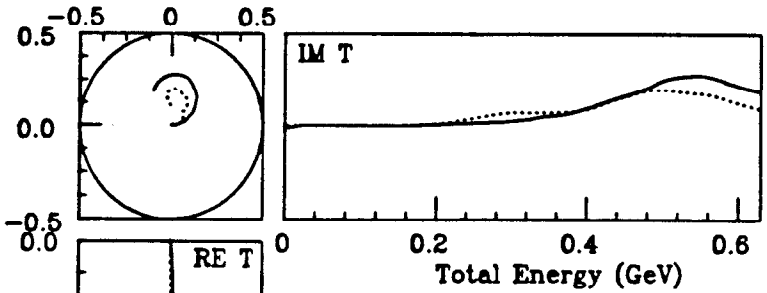

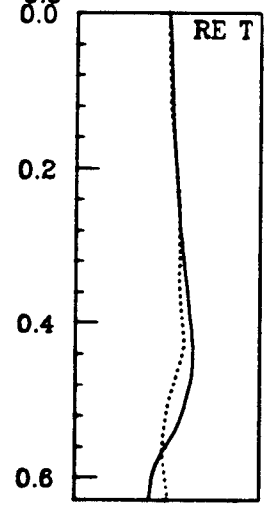

$$FF37 \quad vs. \quad \frac{7}{6\sqrt{6}} \cdot FF15 + \frac{2}{3}\sqrt{\frac{5}{3}} \cdot FF35$$

FIG. 6b

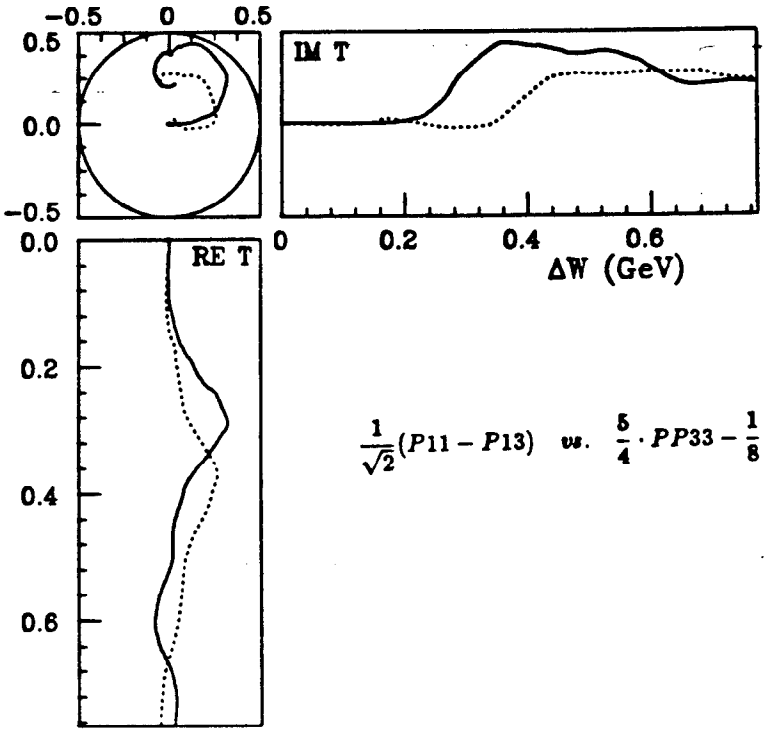

FIG. 7a

$$\frac{1}{\sqrt{2}}(P11 - P13) \quad vs. \quad \frac{5}{4} \cdot PP33 - \frac{1}{8} \cdot PP11$$

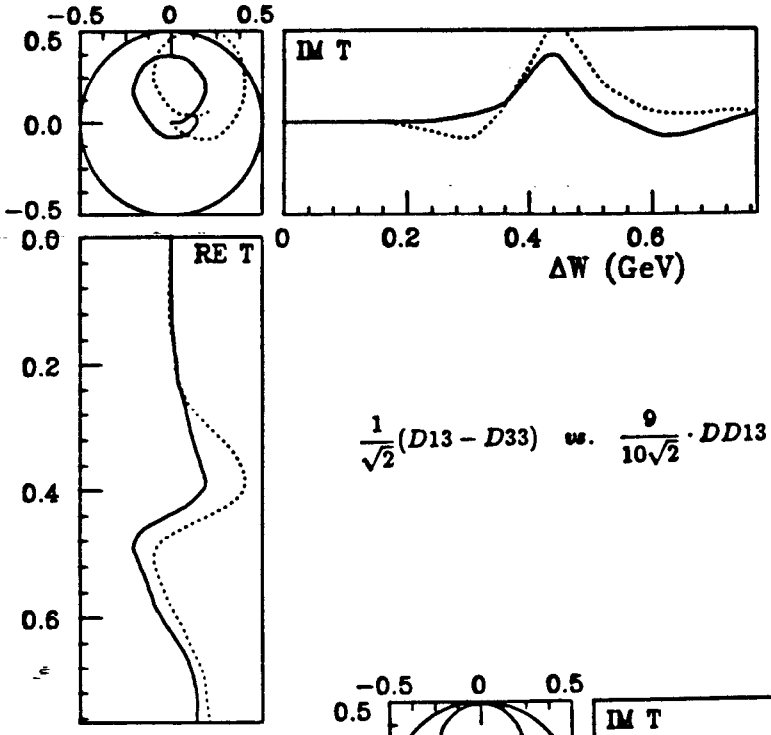

FIG. 7b

$$\frac{1}{\sqrt{2}}(D13 - D33) \quad vs. \quad \frac{9}{10\sqrt{2}} \cdot DD13 + \frac{9\sqrt{7}}{20} \cdot DD15$$

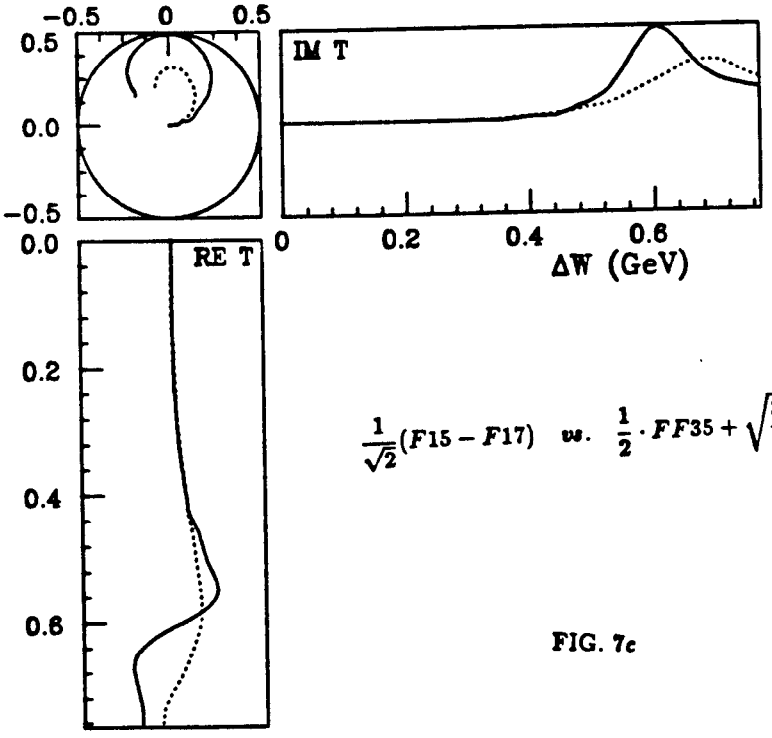

$$\frac{1}{\sqrt{2}}(F15 - F17) \quad vs. \quad \frac{1}{2} \cdot FF35 + \sqrt{\frac{3}{5}} \cdot FF37$$

FIG. 7c